NAVAL POSTGRADUATE SCHOOL

MONTEREY, CALIFORNIA

THESIS

EXPERIMENTAL EVALUATION OF DEWAR VOLUME AND COLD FINGER SIZE IN A STIRLING CRYOCOOLER LIQUID AIR ENERGY STORAGE (LAES) SYSTEM

by

Howard M. Swanson Jr.

June 2021

Thesis Advisor:	Anthony G. Pollman
Co-Advisor:	Alejandro S. Hernandez
Second Reader:	Gary W. Parker

THIS PAGE INTENTIONALLY LEFT BLANK

REPORT DOCUMENTATION PAGE				*Form Approved OMB No. 0704-0188*
Public reporting burden for this collection of information is estimated to average 1 hour per response, including the time for reviewing instruction, searching existing data sources, gathering and maintaining the data needed, and completing and reviewing the collection of information. Send comments regarding this burden estimate or any other aspect of this collection of information, including suggestions for reducing this burden, to Washington headquarters Services, Directorate for Information Operations and Reports, 1215 Jefferson Davis Highway, Suite 1204, Arlington, VA 22202-4302, and to the Office of Management and Budget, Paperwork Reduction Project (0704-0188) Washington, DC 20503.				
1. AGENCY USE ONLY ***(Leave blank)***	**2. REPORT DATE** June 2021	**3. REPORT TYPE AND DATES COVERED** Master's thesis		
4. TITLE AND SUBTITLE EXPERIMENTAL EVALUATION OF DEWAR VOLUME AND COLD FINGER SIZE IN A STIRLING CRYOCOOLER LIQUID AIR ENERGY STORAGE (LAES) SYSTEM				**5. FUNDING NUMBERS** RMNPB
6. AUTHOR(S) Howard M. Swanson Jr.				
7. PERFORMING ORGANIZATION NAME(S) AND ADDRESS(ES) Naval Postgraduate School Monterey, CA 93943-5000				**8. PERFORMING ORGANIZATION REPORT NUMBER**
9. SPONSORING / MONITORING AGENCY NAME(S) AND ADDRESS(ES) Office of Naval Research				**10. SPONSORING / MONITORING AGENCY REPORT NUMBER**
11. SUPPLEMENTARY NOTES The views expressed in this thesis are those of the author and do not reflect the official policy or position of the Department of Defense or the U.S. Government.				
12a. DISTRIBUTION / AVAILABILITY STATEMENT Approved for public release. Distribution is unlimited.				**12b. DISTRIBUTION CODE** A

13. ABSTRACT (maximum 200 words)

This paper uses an experimental approach to evaluate two design characteristics for a liquid air energy storage (LAES) and generation system as part of the verification and validation of system component design for a microgrid power system. The LAES subsystem evaluated utilized a Stirling engine–based cryocooler that employs a cold finger placed into Dewar, which allows the pumping of heat out of a Dewar. As the heat is pumped out, the air temperature in the Dewar cools to below the condensation point and the air in the Dewar liquifies and is stored in the Dewar. Using a design of experiments, the cold finger surface area and Dewar volume were evaluated to determine the criticality and significance of changing their dimensions on the total liquid air production mass and average liquid air production rate during the experiments. This analysis found that changing the surface area of the cryocooler cold finger was a statistically significant design characteristic that affected total liquid air production and average production rate while changing the volume of the Dewar was not statistically significant. Additional responses relative to the time when the first gram of liquid air was produced and the minimum cold tip temperature that the cryocooler was able to achieve provided additional insight into design characteristics that can be used to inform the engineer when making design tradeoffs for specific microgrid operational environments.

14. SUBJECT TERMS liquid air energy storage, LAES, Dewar, vacuum insulated container, Stirling, cryocooler, renewable energy, micro-grid			**15. NUMBER OF PAGES** 81
			16. PRICE CODE
17. SECURITY CLASSIFICATION OF REPORT Unclassified	**18. SECURITY CLASSIFICATION OF THIS PAGE** Unclassified	**19. SECURITY CLASSIFICATION OF ABSTRACT** Unclassified	**20. LIMITATION OF ABSTRACT** UU

NSN 7540-01-280-5500 Standard Form 298 (Rev. 2-89) Prescribed by ANSI Std. 239-18

THIS PAGE INTENTIONALLY LEFT BLANK

Approved for public release. Distribution is unlimited.

EXPERIMENTAL EVALUATION OF DEWAR VOLUME AND COLD FINGER SIZE IN A STIRLING CRYOCOOLER LIQUID AIR ENERGY STORAGE (LAES) SYSTEM

Howard M. Swanson Jr.
Lieutenant Colonel, United States Army
BS, U.S. Military Academy, 2004

Submitted in partial fulfillment of the
requirements for the degree of

MASTER OF SCIENCE IN SYSTEMS ENGINEERING

from the

NAVAL POSTGRADUATE SCHOOL
June 2021

Approved by: Anthony G. Pollman
Advisor

Alejandro S. Hernandez
Co-Advisor

Gary W. Parker
Second Reader

Ronald E. Giachetti
Chair, Department of Systems Engineering

THIS PAGE INTENTIONALLY LEFT BLANK

ABSTRACT

This paper uses an experimental approach to evaluate two design characteristics for a liquid air energy storage (LAES) and generation system as part of the verification and validation of system component design for a microgrid power system. The LAES subsystem evaluated utilized a Stirling engine–based cryocooler that employs a cold finger placed into Dewar, which allows the pumping of heat out of a Dewar. As the heat is pumped out, the air temperature in the Dewar cools to below the condensation point and the air in the Dewar liquifies and is stored in the Dewar. Using a design of experiments, the cold finger surface area and Dewar volume were evaluated to determine the criticality and significance of changing their dimensions on the total liquid air production mass and average liquid air production rate during the experiments. This analysis found that changing the surface area of the cryocooler cold finger was a statistically significant design characteristic that affected total liquid air production and average production rate while changing the volume of the Dewar was not statistically significant. Additional responses relative to the time when the first gram of liquid air was produced and the minimum cold tip temperature that the cryocooler was able to achieve provided additional insight into design characteristics that can be used to inform the engineer when making design tradeoffs for specific microgrid operational environments.

THIS PAGE INTENTIONALLY LEFT BLANK

TABLE OF CONTENTS

THIS PAGE INTENTIONALLY LEFT BLANK

LIST OF FIGURES

LIST OF TABLES

THIS PAGE INTENTIONALLY LEFT BLANK

LIST OF ACRONYMS AND ABBREVIATIONS

DOD	Department of Defense
DOE	Design of Experiments
LAES	Liquid Air Energy Storage
NPS	Naval Postgraduate School
PV	Pressure Volume
RTD	Resistance Temperature Detector
TPL	Turbo-Propulsion Laboratory

THIS PAGE INTENTIONALLY LEFT BLANK

EXECUTIVE SUMMARY

As military equipment, planning, and operations have become more digitized and technology driven, the demand for a continuous electrical supply has grown. This demand has been traditionally answered with diesel generators, batteries, or a reliance on local electrical distribution systems. These traditional methods reduce the Department of Defense's (DOD) energy resilience through the increased logistical burden for transporting fossil fuels to supply generators and through the reliance on local infrastructure that is often outside of military control (Narayanan et al. 2020). Additionally, the transportation of fuel in combat zones is a critical vulnerability to combat forces that has resulted in significant casualties in recent conflicts in Iraq and Afghanistan (Pollman 2013).

Localized generation of energy by renewable resources through islanded microgrids directly addresses this problem by reducing the logistical burden on forces for a continual supply of petroleum and removing the reliance on local electrical infrastructure eliminating critical vulnerabilities to military operations. However, a significant consideration for mobile military applicable renewable energy generation resources such as wind and solar power is that these systems often suffer from intermittent generation based on when the sun is shining or when the wind is blowing. Intermittent generation requires a mechanism to store excess energy during times of high production for use when generation is not available or to move available power from periods of low demand to high demand times to support a continuous electrical supply (Hawxhurst et al. 2017). A potential energy storage solution for deployable military units using microgrids is the use of liquid air energy storage (LAES).

LAES systems can work through several different processes; however, the general concept is to use electricity to operate machinery that cools ambient air below its condensation point which causes the air to liquefy. As the air liquefies, it is contained in a Dewar, which is a vacuum insulated container. This liquid air can then be stored and later used to generate electric power through different means such as heating and expanding the liquid air into a gas which is run through a turbine or by the use of a temperature differential utilizing a Stirling engine. LAES is an appealing solution over more common forms of

energy storage such as batteries, capacitors, compressed air, or pumped hydro due to several factors. Liquid air has high energy density, high round trip efficiency potential, lack of geographical limitations, and low technological and safety risks due to its use of standard industrial components from the power and gas industry (Morgan 2016).

This thesis uses an experimental approach to evaluate two design characteristics for a LAES and generation system as part of the system engineering verification and validation of the system component design for a microgrid power system being studied at the Naval Postgraduate School. The LAES subsystem evaluated utilizes a Stirling engine–based cryocooler that employs a cold finger placed into a Dewar, which allows the pumping of heat out of a Dewar. As the heat is pumped out, the air temperature in the Dewar cools to below the condensation point, and the air in the Dewar liquifies and is stored in the Dewar. Using a design of experiments, the cold finger surface area and Dewar volume were evaluated to determine the criticality and significance of changing their dimensions on the total liquid air production mass and average liquid air production rate.

Analysis of data obtained in a two-factor design of experiment found that changing the surface area of the cryocooler cold finger was a statistically significant design characteristic that affected the total liquid air production and the average production rate, while changing the volume of the Dewar was not statistically significant. Additional responses relative to the time when the first gram of liquid air was produced and the minimum cold tip temperature that the cryocooler was able to achieve provided additional insight into design characteristics that can be used to inform the engineer when making design tradeoffs for specific operational environments. Future work on the LAES systems should include replication to confirm statistical validity, incorporation of a control system to optimize the generation of liquid air production based on environmental conditions or forecasts, and continued improvements of the cold finger extension design and testing beyond the design analyzed in this work.

References

Hawxhurst, Kevin, Joshua Williams, Anthony Pollman, and Anthony Gannon. 2017. "Renewable-Powered HVAC with Thermal Storage." *ASHRAE Journal* 59 (12): 21–27.

Morgan, R. E. 2016. "Liquid Air Energy Storage – from Theory to Demonstration." *International Journal of Environmental Studies* 73 (May): 469–80. https://doi.org/10.1080/00207233.2016.1189741.

Narayanan, Anu, Jonathan Welburn, Benjamin Miller, Sheng Li, and Aaron Clark-Ginsberg. 2020. *Deterring Attacks Against the Power Grid: Two Approaches for the U.S. Department of Defense*. RAND Corporation. https://doi.org/10.7249/RR3187.

Pollman, Anthony G. 2013. "Energy Optimization: A Combat Multiplier." *Marine Corps Gazette*, November 2013.

THIS PAGE INTENTIONALLY LEFT BLANK

ACKNOWLEDGMENTS

Thank you, Dr. Pollman and Dr. Hernandez, for the support and mentorship throughout this effort. Your clear guidance and direction were much appreciated.

THIS PAGE INTENTIONALLY LEFT BLANK

I. INTRODUCTION

A. MOTIVATION

Electrical production, distribution, and storage is a critical aspect of most modern military operations that has been mired in the traditional reliance on batteries and diesel generators. As military equipment, planning, and operations have become more digitized and technology driven, the demand for continuous electrical connections have grown. This has induced a significant logistical burden on the Department of Defense (DOD) for supplying the energy demands for operational bases that typically comes from fossil fuel generation such as diesel generators (Pollman 2013). Alternatively, military forces can utilize the local electrical grid for primary power, but this places a significant reliance on a resource that is typically outside of military control (Narayanan et al. 2020). This reliance on petroleum logistics or local electrical grids reduces the energy resilience of DOD forces especially when deployed around the world or in combat zones. Localized generation of energy by renewable resources as part of an islanded microgrid that can be disconnected from the larger electrical grid directly address this problem.

Microgrids are energy generation and distribution systems of varying types that provide electricity at a small scale. These microgrids can operate independently or in unison with a larger electrical grid system. When set up as an islanded microgrid, which is completely separate from a local electrical grid, or as an integrated system with a local electrical grid, microgrids support DOD energy resilience by allowing either backup operation when the main power grid is down or standalone operations completely disconnected from the grid (Narayanan et al. 2020). Combining microgrids with renewable energy generation options further enhances the energy resilience by removing the dependence on petroleum products. This setup of a renewable energy microgrid, therefore, has the potential to provide continuous electrical supply to DOD forces through significantly less vulnerable means and provides the possibility to create a portable system that can be deployable with mobile forces.

A significant consideration for renewable energy generation resources that are mobile, such as wind and solar power, is that these systems often suffer from intermittent generation based on when the sun is shining or when the wind is blowing. This requires a mechanism to store excess energy during times of high production for use when generation is not available or to move available power from periods of low demand to high demand times to support a continuous electrical supply (Hawxhurst et al. 2017). Many methods exist to store excess electrical energy which include capacitors, batteries, hydro pumping, compressed air, and mechanical storage such as flywheels to name just a few of the possibilities (Ibrahim, Ilinca, and Perron 2008). Each of these technologies vary on the spectrum of power capacity relative to energy storage duration, as shown in Figure 1, which makes them viable options for energy storage application.

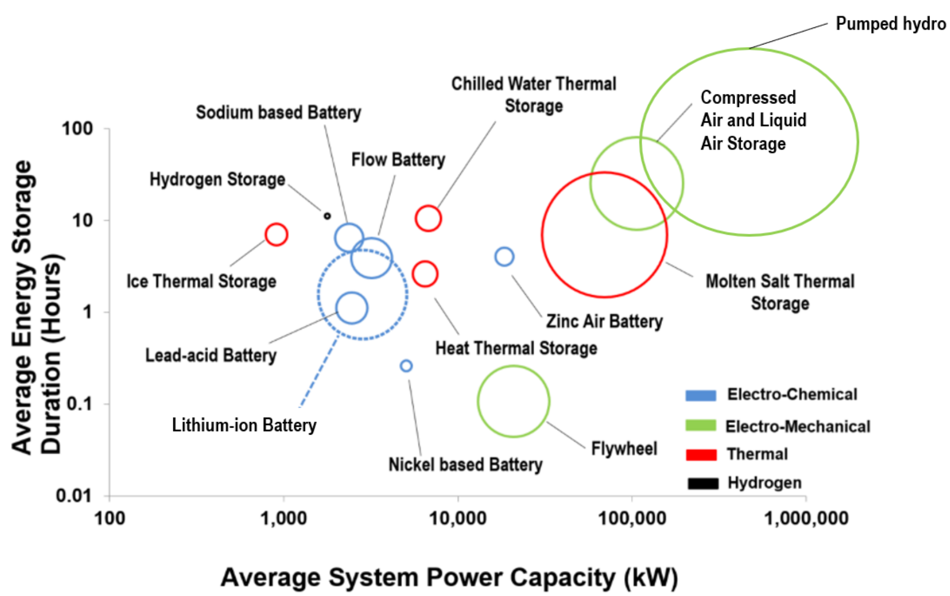

Figure 1. Energy Storage Technologies. Adapted from Fu, Remo, and Margolis (2018).

However, each of these methods have significant disadvantages when used in mobile military operations due to a variety of reasons ranging from weight to geographical requirements (Ibrahim, Ilinca, and Perron 2008). A potential energy storage solution for deployable military units using microgrids is the use of liquid air energy storage (LAES).

B. BENEFIT

This research benefits the DOD strategically because the DOD is the largest federal governmental consumer of energy, spending approximately 2% of its annual budget on energy (Greenley 2019). This energy consumption is broken down into two divisions with the first being installation energy for fixed installations and non-tactical vehicles consuming 30% of the total DOD energy demands (Greenley 2019). The second division being operational energy for sustaining military forces, weapon platforms, and military operations in which 70% of DOD energy demands are consumed (Greenley 2019). Microgrids can address DOD's installation energy needs by providing them primary or backup power; microgrids can also address operational energy needs by providing deployable power options. The use of microgrids, therefore, has the potential to strategically impact military operations, turning energy generation into a combat multiplier rather than a logistical burden to commanders (Pollman 2013).

Additionally, the DOD's energy investment priorities focus on energy resilience and conservation (Jung 2020). Incorporating renewable energy generation and storage into a microgrid addresses current DOD priorities by providing an alternate mean of generation that is not reliant on the logistical considerations of transporting fossil fuels nor vulnerable to uncontrolled local electrical grid vulnerabilities and intermittent operations. The use of renewable energy generation also provides operational and tactical benefits as there is a positive correlation to the fuel consumed by the U.S. military during combat operations and casualties incurred (Wald and Captain 2009). This vulnerability is highlighted by the success that U.S. adversaries in Iraq and Afghanistan have had in disrupting U.S. energy supply chains by targeting fuel convoys historically accounting for 10–12% of all casualties (Eady et al. 2009). Therefore, this research provides potential DOD casualties reductions and cost savings through reduced energy purchasing requirements, additional energy generation options for deployable forces, and increased energy resilience through reduced logistical needs and reduced reliance on local infrastructure.

C. BACKGROUND

The Naval Postgraduate School (NPS) has been conducting ongoing research into islanded microgrids as a means to support the DOD's initiatives for expeditionary energy solutions and for energy resilience. The Turbo-Propulsion Laboratory (TPL) at NPS is at the forefront of this effort and currently uses a combination of wind and solar power resources to generate electrical power (Gannon 2017). This experimental microgrid laboratory is designed to evaluate the possibilities of modular microgrid structures and technologically innovative solutions for microgrid power generation and storage (Pollman and Gannon 2015).

Past systems for storing excess energy at the TPL have evaluated traditional batteries, capacitors, compressed air storage and thermal storage. As a mobile and deployable solution for the DOD, batteries are not ideal due to either their high weight with legacy battery technology or the use of limited and exotic materials when modern battery technology is employed. Capacitors alternatively suffer from the inability to slowly discharge and provide a source of power over an extended period (Gannon 2018). Thermal storage proves promising for heating and cooling systems but does not address electrical demand (Hawxhurst et al. 2017).

An evaluation of alternative methods to store energy has indicated that the emerging technology of LAES could be a particularly promising application for storing and subsequently recovering excess electrical energy. Liquid air has high energy density, high round trip efficiency potential, lack of geographical limitations, and low technological and safety risks. In comparison to using compressed air as an energy storage mechanism, Wang et al. (2015) found that liquid air has an energy density of 296.6 kJ/Liter while compressed air at 200 bar only had an energy density of 70.07 kJ/Liter. Krawczyk et al. (2016), found that LAES systems are also capable of higher round trip efficiencies than a compressed air energy storage system. Furthermore, liquid air systems are not geographically limited like pumped hydro systems that require water access, large storage lakes, and a nearby elevation differential (Kim et al. 2012). Finally, LAES is an appealing solution due to its use of standard industrial components from the power and gas industry which reduces integration, production, and operational risk due to their technological maturity along with the low working pressures of LAES that mitigate many safety considerations with high pressure energy storage systems (Morgan 2016).

Previous work at NPS has focused on modeling LAES, thermodynamic analysis, functional analysis, and component selection. The work on liquid air generation and storage has been split into two efforts. The first utilized the Linde-Hampson cycle to produce liquid air, and the second used a Stirling engine cryocooler. Howe (2018) presented a method for calculating the work done by a compressor and the liquid air yield in a Linde-Hampson system at NPS. The author also presented an energy analysis of LAES with an examination of the ideal operating ranges and trade space in a Linde-Hampson LAES system design. Howe, Pollman, and Gannon (2018) identified the ideal energy and exergy efficiency for a Linde-Hampson cycle liquefaction system while evaluating system components that would have the greatest impact on energy and exergy. Willis (2019) used industrial process modeling and simulation software, Aspen HYSYS, to model a Linde-Hampson cycle system for a building sized system to generate a parametric model for application into the NPS microgrid system. A model based system's engineering approach was then applied by Amalla (2019) to recommend improvements to the Linde-Hampson system through changes in the heat exchanger design. Functional requirements were established by Bailey (2019) along with an examination of significant system factors. Modeling and simulation was also used by Girouard, Pollman, and Hernandez (2019) to determine commercial components that could be used to prototype a new Linde- Hampson system at the TPL. Girouard (2019) also evaluated a Stirling cryocooler system assessing LAES container design and establishing an empirical relationship for liquid air generation based on system input power and container volume. Finally, Bailey, Pollman, and Paulo (2020) examined the used of dual Stirling engines for generation and recovery of liquid air energy where experimentation allowed the comparison against an ideal Stirling cycle and the calculation of energy recovery. Building off these previous efforts, this thesis seeks to expand on these previous works and contribute to the ongoing microgrid and LAES work at NPS by examining system design impacts to the Stirling engine based cryocooler generation process.

D. PROBLEM EXAMINATION

As a relatively new energy storage technology, significant challenges with LAES still need to be addressed to increase its efficiency and make it a viable option relative to other traditional energy storage mechanisms. Analysis of previous research results on the creation of liquified air for an islanded microgrid system at NPS has shown a consistent but low production of liquified air when using a Stirling cycle based cryocooler. Low production constrains the amount of energy that can be stored and later recovered as electrical energy. It is hypothesized that the limiting factor in the production of liquid air using the setup later discussed in this thesis was due to the limited cold surface area available to interact with gaseous air and convert into liquid air. Therefore, an evaluation of system elements relative to the size of the cryocooler's cold finger and the size of the liquid air production Dewar, which is a vacuum insulated container, seeks to determine if these are critical factors and their relative impact on system performance.

E. SYSTEMS ENGINEERING RELEVANCE

The goal of this effort is to support the engineer's understanding of the constraints or boundaries of the liquid air generation and storage components used for the proposed microgrid. This effort is conducted in alignment with the systems engineering V model as outlined by Forsberg and Mooz (1992) and shown in Figure 2. The V model is a system engineering process model that begins with a need in the top left which is decomposed and defined to develop hardware/software. The model then progresses through an integration and verification sequence to arrive at a fully operational system.

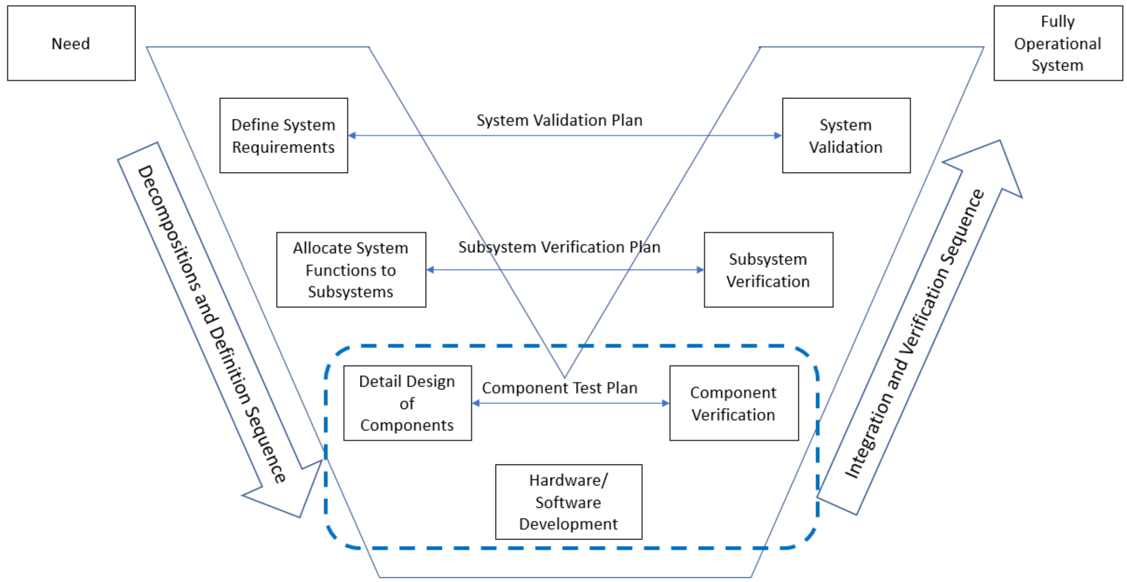

Figure 2. Systems Engineering V-Model.
Adapted from Forsberg and Mooz (1992).

This thesis works within the bottom of the V model, as outlined by the dashed line in Figure 2, with the goal to develop the design details of the liquid air production cryocooler and storage component and implement this design into a subsystem hardware development solution. This thesis effort tests this hardware to verify that components meet the design details before progressing higher in the V model. The proposed hardware solutions that are evaluated differ in two design aspects with the first being the cryocooler's cold finger size and the second being the size of the liquid air production Dewar. A test plan for these designs is laid out using a design of experiments to evaluate how changes in these factors and/or two-way interactions between factors will affect important system output measures. The analysis of this data supports improved efficiency and integration into the completed microgrid system.

THIS PAGE INTENTIONALLY LEFT BLANK

II. EXPERIMENTATION

This thesis documents an experimental approach to gather evidence and answer the proposed research problem. This approach addresses if increasing the surface area of the Stirling cycle based cryocooler's cold finger affects the average production rate and total volume of liquid air production measured as mass. Supporting this analysis was an evaluation of the minimum cold finger temperature that can be achieved by the cryocooler along with the elapsed time to when the system creates its first gram of liquid air. Experiments were conducted using a similar setup to the one used in previous work conducted at NPS and documented in the thesis "Model-Based and Experimental Analysis for Future Liquid Air Energy Storage Systems" to ensure consistency in analysis as this research builds on previous efforts and supports future development of microgrid structures at the NPS TPL (Girouard 2019).

A. CONCEPT

LAES systems work through several different processes; however, the general concept uses electricity to operate machinery that cools ambient air below its condensation point which causes the air to liquefy. As the air liquefies, it is contained in a vacuum insulated container. This liquid air can then later be used to generate electric power through different means such as heating and expanding the liquid air into a gas that is run through a turbine or by the use of a temperature differential using a Stirling engine. Functional modeling of a LAES system provides a structured depiction of the functions, activities, and processes as shown in Figure 3.

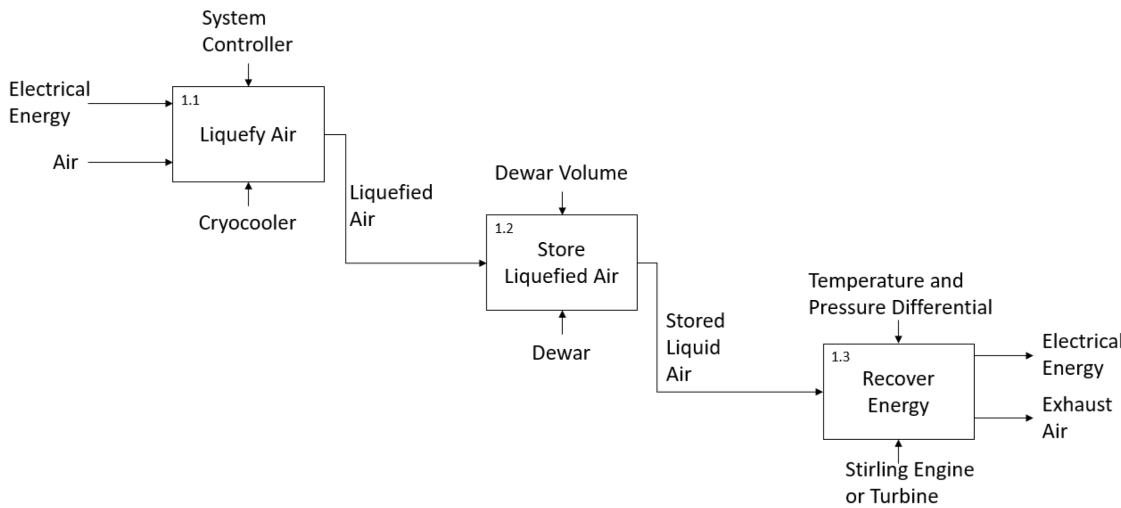

Figure 3. IDEF0 Functional Model for LAES System

This figure shows that the three primary functions of LAES are the creation of liquid air, the storage of liquid air, and the recovery of energy from the liquid air. In this thesis, the mechanism for generating liquid air is a Stirling cryocooler. For the function of storing liquid air the mechanism is a Dewar, and the function of recovering electrical power from this system is not evaluated as this part of the system is outside the scope of the problem statement.

The Stirling engine was conceived by Robert Stirling in 1816. This engine is typically an external combustion, closed-cycle, regenerative heat engine where the working gas is contained within the system and heat energy is converted to mechanical work. The process works through the Stirling cycle which consists of four phases. In the first stage, the gas is compressed in the cold section. It is then moved to the hot section where heat is applied to raise the temperature and expand the gas. The expanding gas works against a piston creating a driving force or work. Finally, the gas is returned to the cold end to start the cycle again. The thermodynamic principle for this operation is shown in the pressure volume (PV) diagram in Figure 4, which consists of isothermal compression (a to b), a isochoric process (b to c), isothermal expansion (c to d), and a isochoric process (d to a) (Shaw 2008).

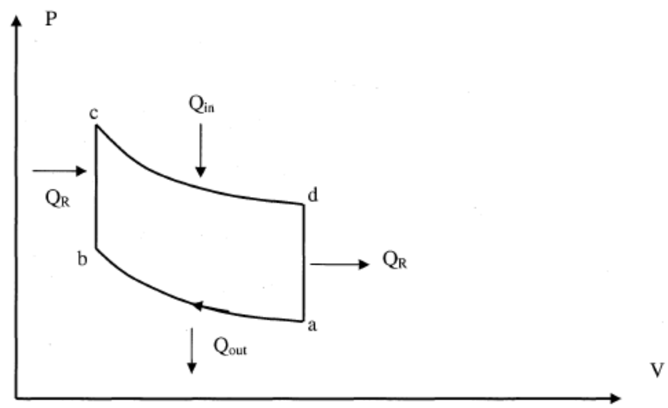

Figure 4. Stirling Cycle PV Diagram. Source: Shaw (2008).

Based off this cycle, the mechanical components vary based on the configuration of the engine but typically consist of a hot and cold end with one or more pistons that drive the fluid between the hot and cold sides and extract work from the system based on a mechanical connection as shown in Figure 5. This engine type is unique in that this system can be reversed to convert mechanical work into a thermal differential thereby creating a heat pump as demonstrated by Philips Research Laboratory in the Netherlands in 1938 (Kohler 1965).

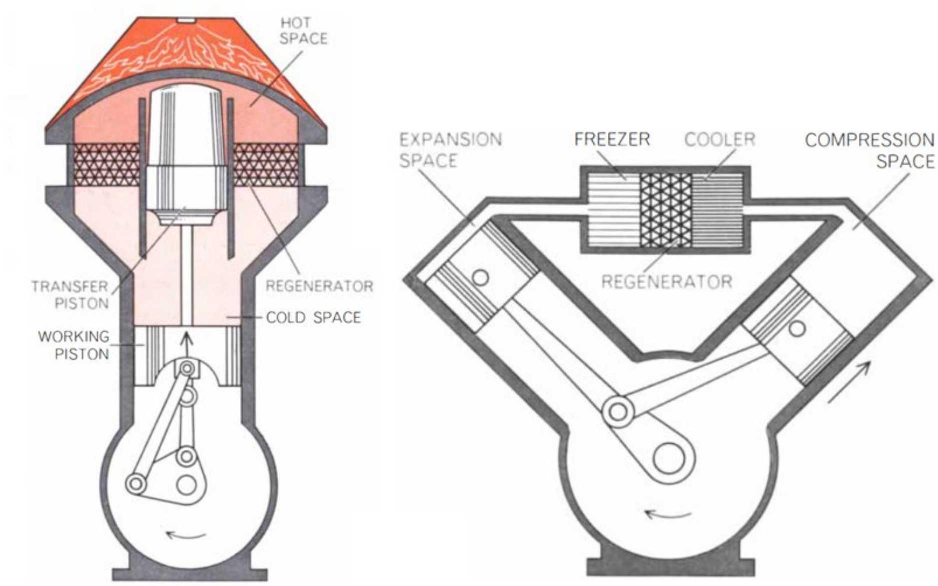

Figure 5. Two Stirling Engine Configurations. Source: Kohler (1965).

By removing the external heat source from the original Stirling engine and driving the system with an external power source, this results in the Stirring cycle continuing to function but in reverse by absorbing heat in the expansion phase (Kohler 1965). This method results in a heat pump, as heat is transferred from the expansion side to the compression side of the engine. Therefore, as a cooling system, this allows for the ability to achieve very low temperatures while having relatively high efficiencies at the temperature necessary to liquify air as shown in Figure 6. This high efficiency results in, theoretically, less energy needed to produce the temperatures necessary to create liquid air, which is important for a microgrid system. This process is the basis for Stirling engine based cryocoolers that allows the expansion side to be placed into an insulated container resulting in the heat, within the container, being pumped out through the cryocooler and into the environment. Therefore, if this container is open for ambient air, then the air within the container will be cooled and condensed into liquid with new air flowing into the container to be cooler and condensed continually as long as work is applied to the system.

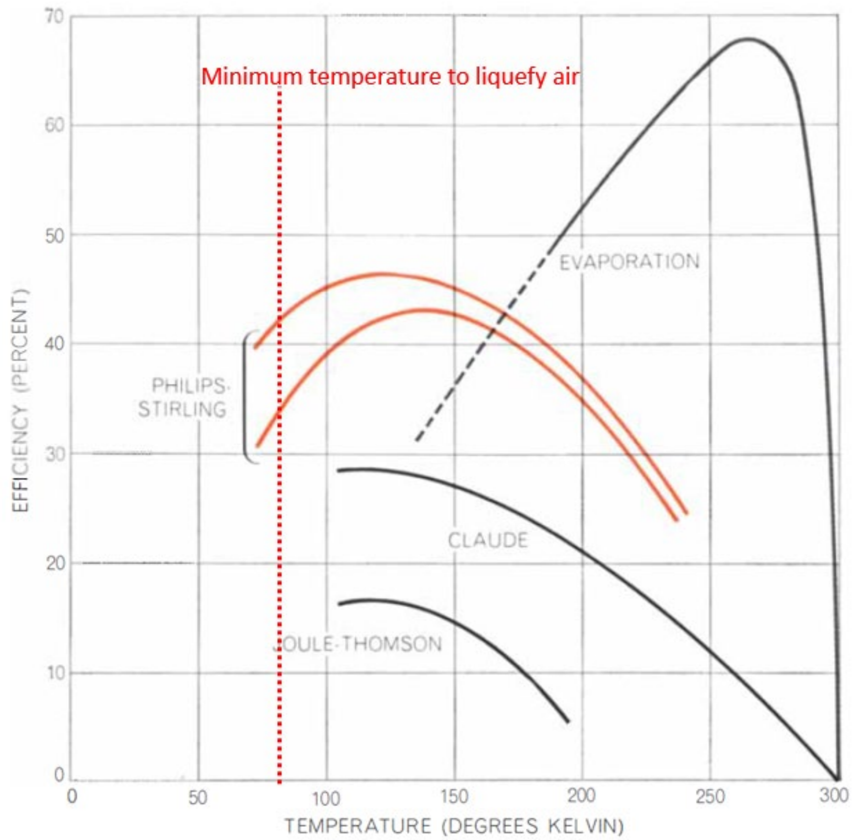

Figure 6. Cooling Efficiencies. Adapted from Kohler (1965).

In order to begin to liquefy air at atmospheric pressure, the temperature must reach at least 81.6 K (Schroeder 2000). This temperature is because air is a mixture of two primary elements being 78% nitrogen and 21% oxygen; therefore, the boiling point will be a temperature between the boiling points of these two elements. Pure oxygen's boiling point is 90.15 K while pure nitrogen has a boiling point of 77 K (Halliday, Resnick, and Walker 2014). Because of this, oxygen condenses sooner than nitrogen, which results in an initially oxygen rich solution as shown in Figure 7.

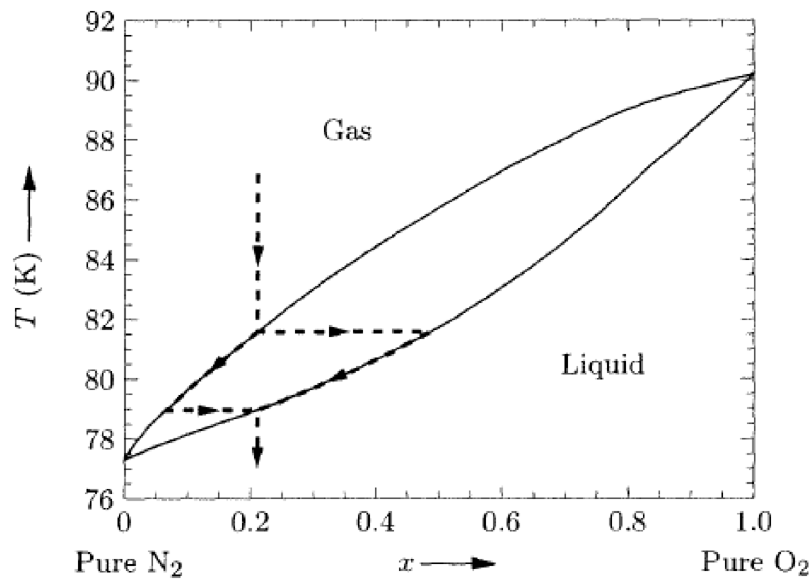

Figure 7. Phase Diagram for Atmospheric Air. Source: Schroeder (2000).

Figure 7 illustrates that as the temperature of the air decreases to 81.6 K as shown by the top vertical line, liquid begins to condense and follows the dotted line to the right. The bottom curve shows that initially the liquid condensing is 48% oxygen as shown on the x axis (Schroeder 2000). As the temperature continues to decrease, "the gas becomes depleted of oxygen and its composition follows the upper curve, down and to the left while the composition of the liquid follows the lower curve" also down and to the left (Schroeder 2000, 194). The continued drop in temperature results in the nitrogen/oxygen ratio increasing back to the original atmospheric ratio once 79.0 K is reached. Therefore, the goal in this experimentation and in a LAES system is to reach and maintain a temperature of 79.0 K to ensure an atmospheric mixture of liquid air.

B. COMPONENTS

The primary component for these experiments is a Stirling cryocooler used to cool the ambient air in a Dewar to the point that the air begins to liquefy. The cryocooler used is a Cryotel GT cryocooler, as shown in Figure 8, which is a commercially available free-piston Stirling engine cryocooler previously purchased for work on liquid air energy generation and storage at NPS. This cryocooler takes electricity and converts it into linear motion for a Stirling engine, which results a thermodynamic cycle that pumps heat from the cold finger at the bottom to the finned radiator at the top (Sunpower Inc. 2016). Heat is then rejected from the cryocooler by a separate fan positioned above the cryocooler to blow ambient air over the cryocooler's radiator fins extending from the hot side of the cryocooler. Attached to the cold finger is a Lake Shore PT-111 Platinum Resistance Temperature Detector (RTD) that reads the resistance and converts this signal into a temperature to allow the monitoring of the cold tip temperature.

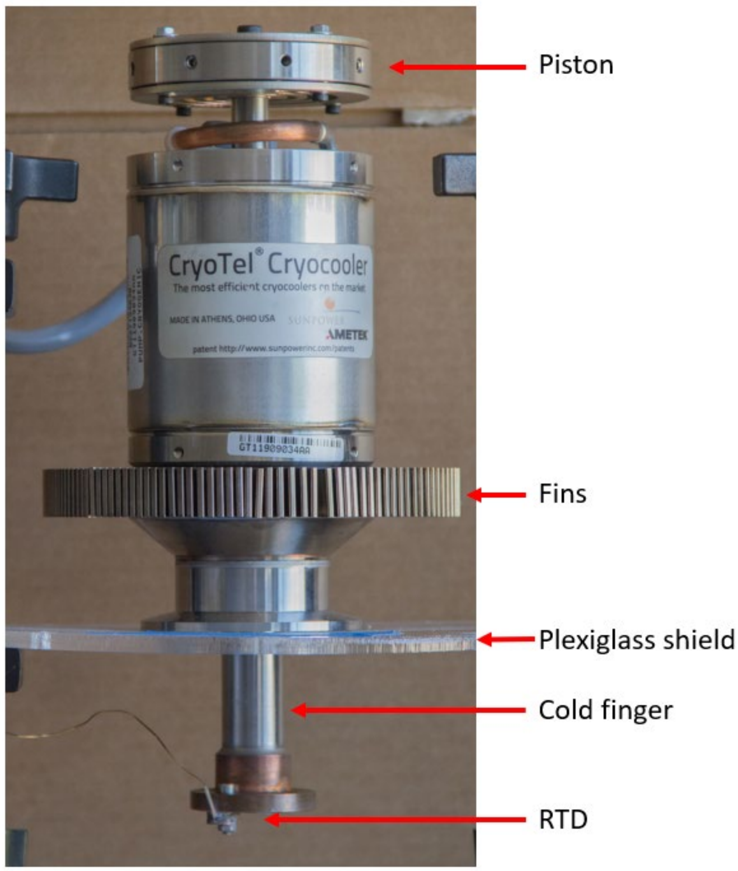

Figure 8. CyoTel GT Cryocooler

The cold finger on the cryocooler consists of an extension with a copper cold tip designed as a mounting flange that allows the cold tip to be secured onto different surfaces. This flange includes four tapped M4 threaded bolt holes that allow the attachment of cylinders of copper used to increase the cold finger's surface area as shown in Figure 9.

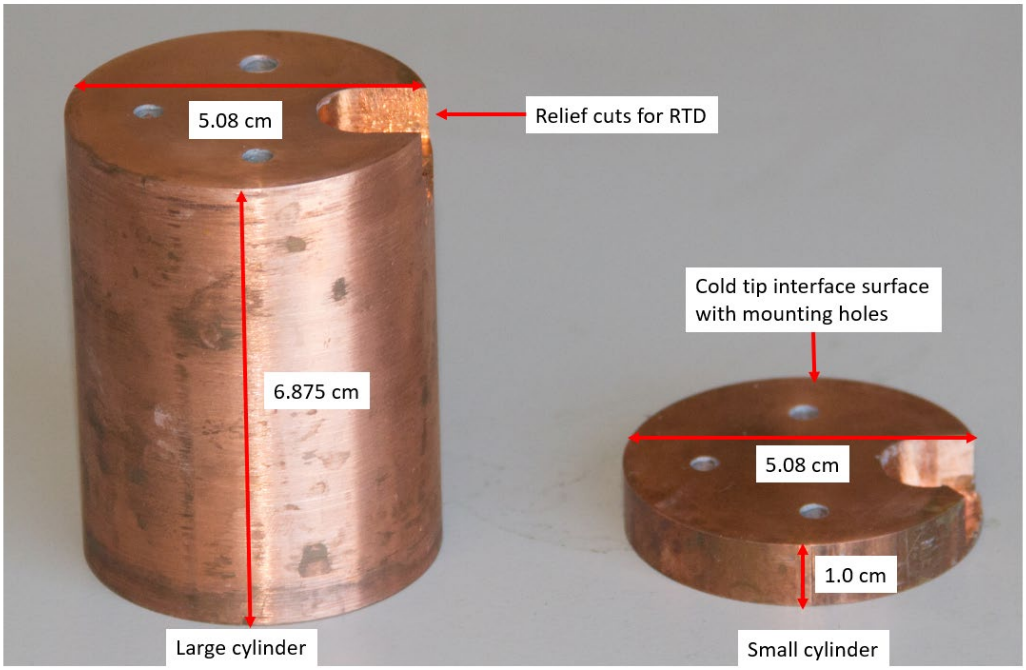

Figure 9. Cold Finger Extension

99.9% pure copper was chosen as the material to increase the surface area of the cold finger based on its high thermal conductivity of 401 W/m*K, which is significantly greater than other commonly available and affordable metals such as steel, brass, or aluminum that range from only 14 to 235 W/m*K (Halliday, Resnick, and Walker 2014). Additionally, because the cold tip is also copper, the incorporation of a copper surface area extension prevents any problems with dissimilar metal during heating/cooling expansions and contractions ensuring constant contact with the cold tip for maximum heat pumping. Consideration was also given to the RTD mounting interface on the cryocooler cold tip by milling minimal and matching reliefs into the copper cylinders so that there would not be any contact between the RTD and the copper cylinders. The relief cut ensures that the cryocooler's feedback loop through the RTD would not be impacted by the addition of each extension and the cryocooler would function the same for all experiments as shown in Figure 10.

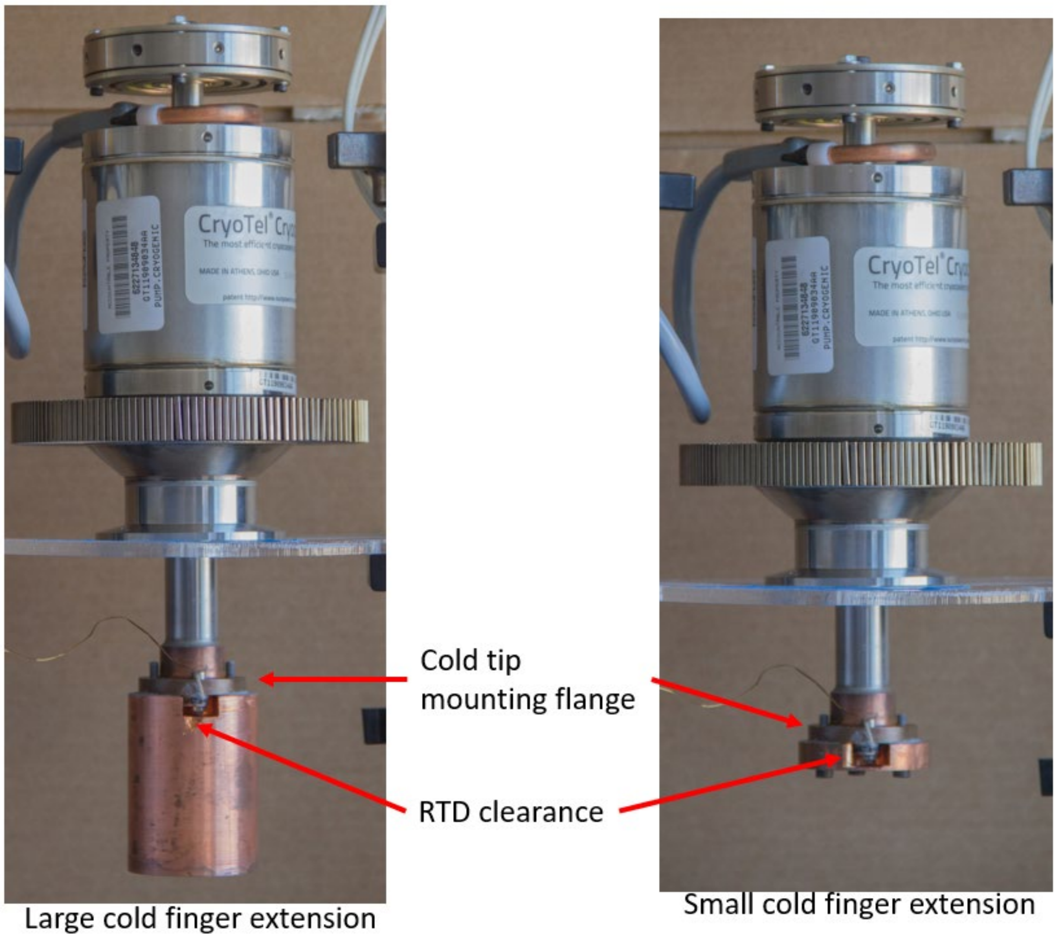

Figure 10. Cold Finger Extensions Mounted on Cryocooler

The Dewars used in the experiments are commercially available vacuum insulated beverage containers that are repurposed for the generation and storage of liquid air by suspending the cryocooler's cold finger within the container. The chosen Dewars are a HydroFlask 354 mL (12 oz) container and a HydroFlask 473 mL (16 oz) container shown in Figure 11. These two Dewars were selected based on several factors. First, previous research at NPS indicated that these Dewars were functional components for producing liquid air (Girouard 2019). Next, they were both made by the same manufacturer and materials, which minimizes variability between production process and designs to minimized uncontrolled experimental factors. Finally, the two sizes allow for the analysis of Dewar size independently while maintaining a constant air volume by proportionally changing the cold finger size.

Figure 11. HydroFlask Dewars

To account for the effect of changing the Dewar's internal volume as the cold finger's surface area is increased, the two copper cylinders were machined to have the same Dewar internal air volume when installed. To accomplish this, the two copper cylinders were machined from the same block of 99.9% pure copper to 5.08 cm in diameter. The small cylinder was machined to a length of 1.0 cm and the large cylinder to 6.875 cm as shown in Figure 9. These efforts resulted in the small cylinder having a volume measurement of 20.3 mL and, when installed into the 354 mL HydroFlask, reduced its internal air volume to 333.7 mL. The large cylinder resulted in a volume measurement of 139.3 mL, which when placed into the 473 mL HydroFlask, reduced its internal air volume to a corresponding 333.7 mL. These cylinders were then drilled to allow three small M4 hex head screws to be used to secure the cold finger extension onto the cryocoolers cold tip. The small cylinder increased the cold finger's surface area by 56.5 cm^2 and the large cylinder by 150.3 cm^2.

Power was supplied to the cryocooler with a TekPower TP6010E DC power supply, rated at 60 volts and 10 amps as shown in Figure 12**,** which is able to provide the maximum power of 240 watts to the cryocooler. Power was delivered using a constant voltage setting of 48 volts with the amperage varying based on system demand.

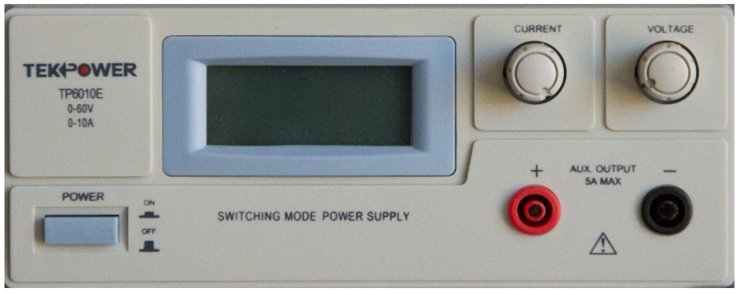

Figure 12. TekPower TP6010E DC Power Supply

System power was monitored by placing a Rcharlance 150A power monitor shown in Figure 13 between the supply and the controller (Rcharlance 2020).

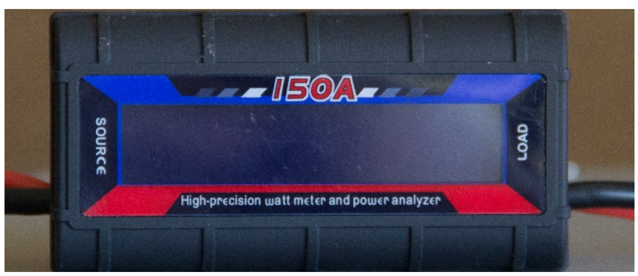

Figure 13. Rcharlance 150A Inline Power Monitor

Controlling the cryocooler was a SunPower Gen II controller shown in Figure 14 that automatically adjusts the power applied to the cryocooler based on the temperature feedback loop from the RTD installed on the cold finger (Sunpower Inc. 2016). The controller was connected using a RS-232 serial communications cable to a desktop computer that allowed the execution of the controller's software interface. The controller's interface allows operating parameters such as power level or desired cold tip temperature to be specified and monitored.

Figure 14. Cryocooler Controller

During these experiments, the desired maximum system power level of 240 watts was set using the user interface and the controller was allowed to adjust and monitor power delivery to the cryocooler to ensure normal safe operation of the equipment while maintaining the desired power output. A power level of 240 watts ensured the system was operating at its maximum design capabilities and the cryocooler was continually working to achieve its minimum temperature of 40 K, therefore, maximizing the heat pumping and possibility for liquid air generation (Sunpower Inc. 2016).

C. SETUP

The components for the experiments were assembled as shown in Figure 15 by first utilizing a large circular plexiglass base approximately 30 cm in diameter to act as the support surface for the cryocooler and wind guard for the Dewar where the liquid air would be produced.

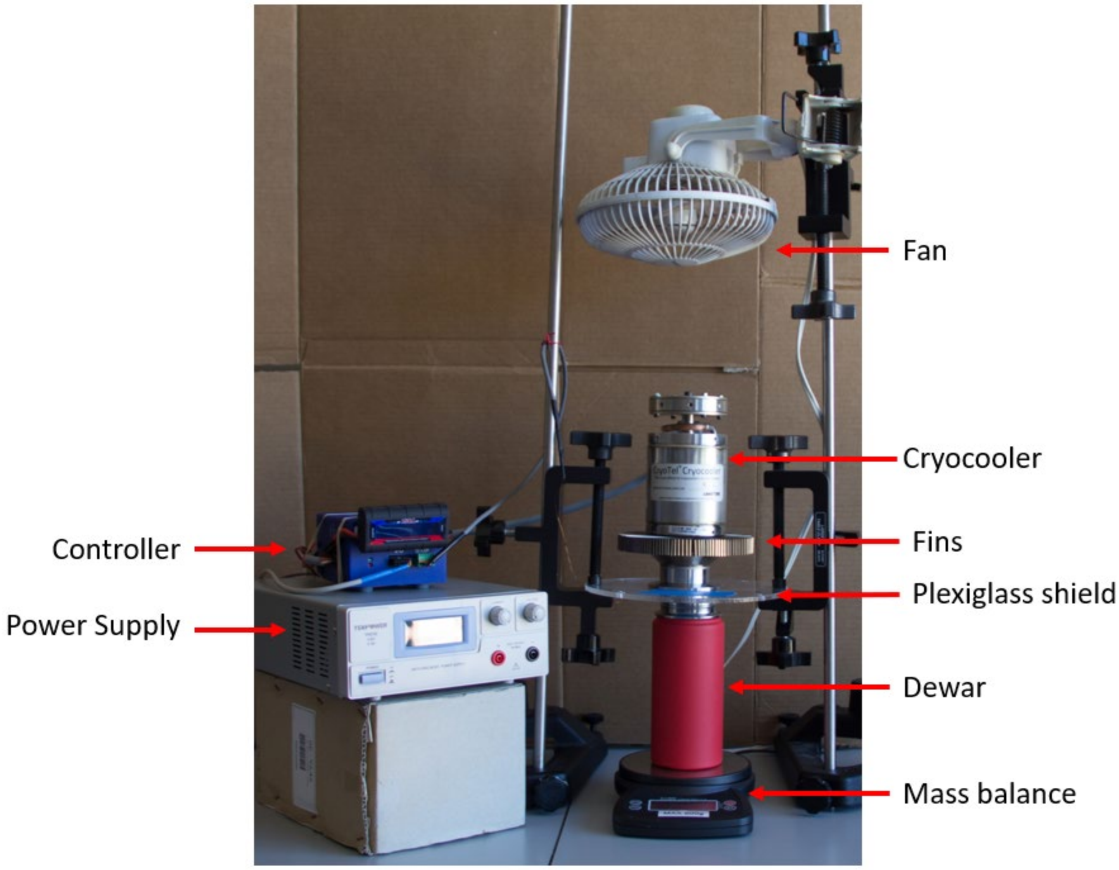

Figure 15. Experimentation Setup

The center of the plexiglass base was cut out just large enough (approximately 7.6 cm) to allow just the cryocooler cold finger to pass through. The flange on the cryocooler then rested on plexiglass allowing the cold finger portion of the cryocooler to extend below the plexiglass base and the plexiglass to support the weight of the cryocooler while physically separating the hot top portion of the cryocooler from the cold bottom portion of the cryocooler as seen in Figure 8. The plexiglass base was then mounted to two laboratory stands with height-adjustable supports to hold the plexiglass base with suspended cryocooler. The RTD was then coated with Corsair TM30 Performance Thermal Paste and attached to one of the four cold tip mounting holes with a hex head bolt. A copper cold finger extension was then coated with the same thermal conductive paste and attached using three hex head screws to the underside of the cryocoolers cold finger's mounting flange as shown in Figure 9.

Below the cryocooler, the Dewar was placed on top of a J Scales J-600 mass balance with a 0.1g precision and 600g capacity (J Scales, 2020). The assembly with the cryocooler was then lowered on the laboratory stands so that the cryocooler's cold finger suspended inside the Dewar without touching the Dewar. An air gap of 0.5 cm was maintained on all experiments between the bottom of the plexiglass plate and the top of the Dewar to allow ambient air to enter the Dewar, be chilled by the cold finger, and condense into liquid air. The liquid air would then drip off the cold finger and be captured in the Dewar with the mass of the changing quantity of liquid air being evaluated using the mass balance on which the Dewar sat.

Above the cryocooler a fan was mounted to the top of one of the laboratory stands. The fan was positioned so that it drove its air vertically downward over the top of the cryocooler. The flow ensured full 360-degree circulation of ambient air past the cryocooler's radially extended and vertically oriented radiator fins. This positioning allowed for the continuous rejection of heat from the cryocooler with the plexiglass blocking this heat from being blown into the vicinity of the Dewar.

The experiment's electronics were setup as shown in Figure 16 by first soldering the RTD's cabling to a 6-socket connector (P/N 277–1434-ND) based on the directions in the cryocoolers instruction manual and connected to the Gen II controller (Sunpower Inc. 2016). The connection provided the cold tip temperature readout, through the system software, and power regulation by the controller through a temperature feedback loop. Next, the cryocooler's two-wire power cable was soldered to the corresponding inline power monitor's wires and then connected to the controller's power output side power wire posts. The plug side of the power cable attached to the cryocooler and was secured with a M3 x 12 socket head cap screw. Finally, a RS-232 serial communications cable with the 14-pin male input/output connector was plugged into the controller and the 9-pin-D connector plugged into a serial interface port on a Windows based desktop computer.

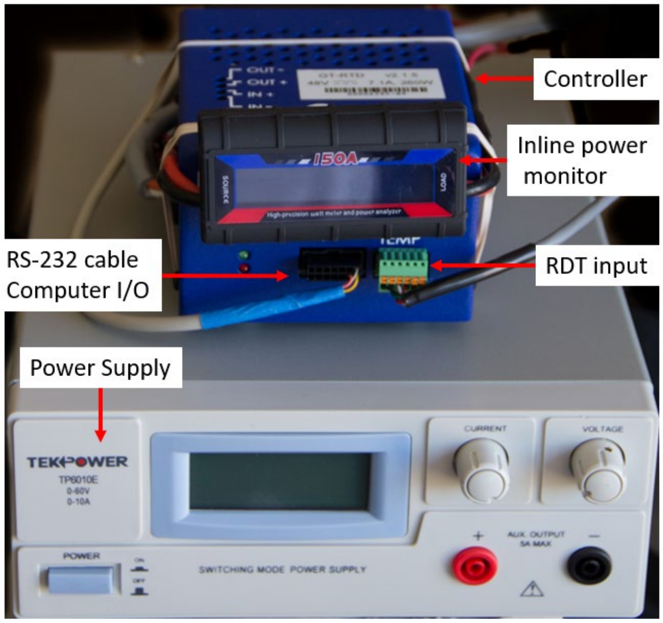

Figure 16. Electronics Setup

The Window's interface for controlling the cryocooler used a free terminal emulation software called PuTTY. After setting the configurations in PuTTY to recognize the controller, the controller was able to be operated with simple programed codes. These codes allow the startup/shutdown of the cryocooler, monitoring of the cold tip temperature, and the setting of desired cold tip temperature or desired power output, which were essential to operating the system and capturing experimental data.

D. PROCEDURES

Each experiment was conducted by starting with a room temperature system. Start conditions required that the cryocooler, cold finger extensions, and Dewar were all the same temperature as the ambient temperature. These temperatures were confirmed with a Sper Scientific 800103 laser thermometer and against the RTD as read through the controller's interface software. Each system was also checked to ensure it was dry and free of any moisture, contaminates, or condensation. Next the selected cold finger extension was installed onto the cold tip with a thin film of thermal paste using hex head bolts. This system was then lowered down the laboratory stands over the selected Dewar resting on the mass balance while ensuring the correct spacing between the plexiglass shield and the top of the Dewar with no contact between the Dewar and cryocooler components.

The cryocooler was then started using the controller interface software. Once the cryocooler was operating, two timers were started. The first timer was used to keep track of the time to first gram of liquid air produced and the second used to keep 10-minute intervals to record the temperature of the cold finger and the mass of the liquid air produced. Each experiment was run for two hours providing 12 data points for the produced liquid air mass on each experiment.

E. DESIGN OF EXPERIMENT

A design of experiments (DOE) was used to produce data that would support the use of traditional statistical techniques. Data was analyzed to produce the quantitative responses of average production rate in grams per minute and the total production of liquid air as measured by mass in grams. A two-level DOE was utilized for this type of analysis that assumes an approximately linear or monotonic response because the intent was to simply determine if the change was significant or not (Law 2015).

The two controllable factors analyzed were Dewar sizes and surface area creating a 2^2 factorial design that generates two levels for each of the two factors. This experimental design is useful for specifically screening out non-critical factors by examining the extreme values for the factor. For the factor of Dewar size, the two levels are the 354 mL and the 473 mL volumes of the two HydroFlasks. The two levels for the cold finger surface area were the small copper cold finger extension with a height of 1 cm and the larger copper cold finger extension with a height of 6.875 cm. These configurations were chosen so that the designs were different enough to stimulate a response but yet not so different that the design parameters were not realistic (Law 2015).

Using the statistical analysis software Minitab, a DOE was prepared using the two-factor, two-level design. Three replications of each design parameter were chosen to increase the sample size available for analysis. Through this, a design matrix was created as shown in Table 1.

Table 1. DOE Design Matrix

StdOrder	RunOrder	CenterPt	Blocks	Finger Size	Dewar Vol
9	1	1	1	Small	354 mL
2	2	1	1	Large	354 mL
10	3	1	1	Large	354 mL
7	4	1	1	Small	473 mL
12	5	1	1	Large	473 mL
1	6	1	1	Small	354 mL
4	7	1	1	Large	473 mL
8	8	1	1	Large	473 mL
5	9	1	1	Small	354 mL
6	10	1	1	Large	354 mL
3	11	1	1	Small	473 mL
11	12	1	1	Small	473 mL

The run order output from Minitab was used to randomize the experimentation to minimize systematic bias due to effects such as changes in environmental conditions (Law 2015). Using this design matrix, each experiment was conducted according to the order and configuration in Table 1 and the experiment setup in Figure 15, then was executed according to the procedures.

THIS PAGE INTENTIONALLY LEFT BLANK

III. RESULTS AND ANALYSIS

The intent of this analysis was to evaluate if the factors of cold finger size and Dewar volume, as independent variables, have a significant effect on the dependent variables of average liquid air production and final mass produced. In addition, the analysis assessed the strength of the independent variables' effect on the dependent variables. Finally, aiding this analysis was an evaluation of supporting factors such as the time to first gram of liquid air produced and the minimum cold tip temperature. This additional assessment helped determine if these factors are significant design considerations in a future LAES system. Therefore, the raw data from the 12 experiments were captured using a spreadsheet program and are listed in Appendix A. The computed data was then transferred over into the DOE design matrix in Minitab as seen in Table 2 for statistical analysis based on a confidence level of 0.95.

Table 2. DOE Data

Finger Size	Dewar Vol	AVG Rate (g/min)	Final Mass (g)	Time to 1st Gram (sec)	Min Tip Temp (K)
Small	354 mL	0.9375	89.7	1487	80.46
Large	354 mL	1.1225	56.9	4225	81.14
Large	354 mL	1.0975	54.9	4231	81.13
Small	473 mL	1.0575	101.8	1340	80.36
Large	473 mL	1.065	53	4323	81.08
Small	354 mL	0.9275	88.2	1453	80.44
Large	473 mL	1.0825	55.2	4186	81.12
Large	473 mL	1.215	67.8	4064	81.04
Small	354 mL	1.0075	102.6	1148	80.40
Large	354 mL	1.08	58.9	3967	81.21
Small	473 mL	1.04	105.2	1187	80.39
Small	473 mL	1.02	102	1294	80.42

The first factor analyzed was the average production rate. This rate was found by averaging the production rate of each experiment over a standardized period of time. Considering that each experiment started producing liquid air at different times due to the different variables in the experiments, a period from 80 to 120 minutes was chosen because all experiments were fully operating during this period. Using this time period, an average production rate over 40 minutes could be equally evaluated across all experiments. From here, a Pareto chart for the average production volume response in grams per min (g/min) was generated to determine critical factors as shown in Figure 17.

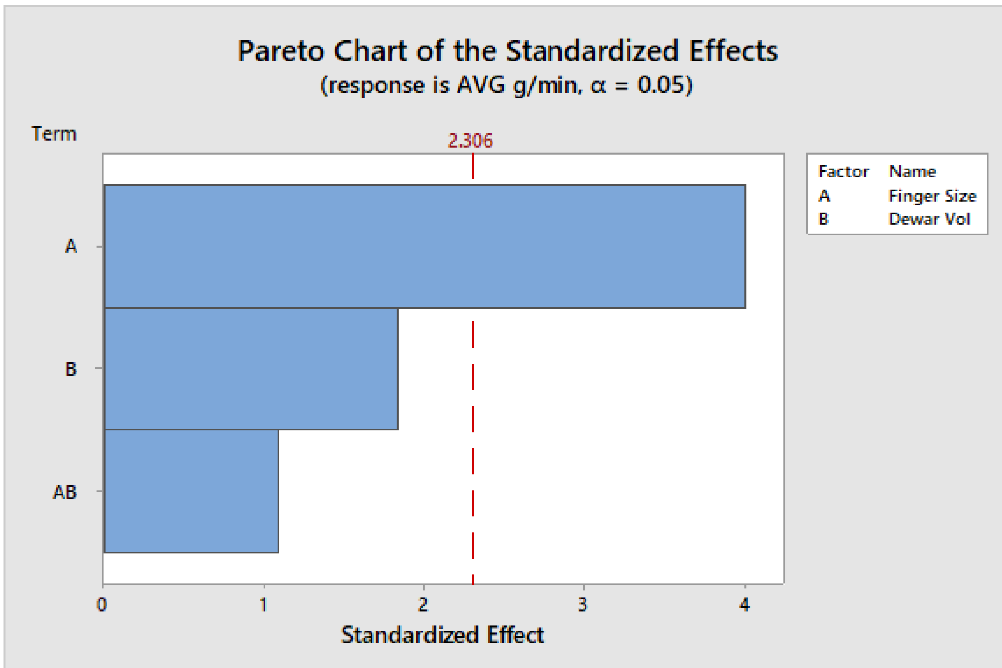

Figure 17. Average Production Pareto Chart

Figure 17 illustrates that the cold finger size was a critical and statistically significant factor in the average production rate of liquid air as it crossed the reference line at 2.306. The other factor of the Dewar volume and the interaction of cold finger size and Dewar volume were not found to be critical factors. For all experiments, a two-way interaction between the factors prove to be insignificant. This evaluation was reinforced with the results of an ANOVA, two-factor with replication, statistical evaluation in Microsoft Excel as shown in Table 3.

Table 3. ANOVA Table for Average Production Rate

ANOVA					
Source of Variation	*SS*	*df*	*MS*	*F*	*P-value*
Finger size	0.03769	1	0.03769	15.9773	0.00397
Dewar Volume	0.00788	1	0.00788	3.34047	0.10501
Interaction	0.00278	1	0.00278	1.17664	0.30965
Within	0.01887	8	0.00236		
Total	0.06721	11			

The ANOVA was used as a simple statistical method for determining whether the main effects and two-way interaction of the two factors were significant to the resultant measures. The ANOVA isolates each factor in a hypothesis test that initially asserts that the mean output measure is the same regardless if the factor value is on one extreme or the other, i.e., the factor has no effect. The alternative is that there is some statistical difference between the measure means. The test statistic is the F-value that results based on the observed data from the experiments. A large F-value results in rejecting the null hypothesis in favor of the alternative hypothesis. For instance, cold finger size results in an F-value of 15.9773. The probability that a value this extreme would be seen if the null hypothesis were true is 0.00397, which we call the p-value. Because this probability is very small, smaller than the significance level chosen, we state that the factor, cold finger size, is statistically significant and will influence the output measure.

To examine the direction of each factor a main effects plot is generated in Minitab as shown in Figure 18. The plot indicates that as both the cold finger size and Dewar volume are increased, there is a positive effect on the average production volume. The cold finger size displays a greater magnitude of change as it is the significant factor. Therefore, if the maximum average production rate of this experimental setup would be desired, the larger cold finger and large Dewar would be selected but only the larger cold finger would have a statistically significant impact on the production rate.

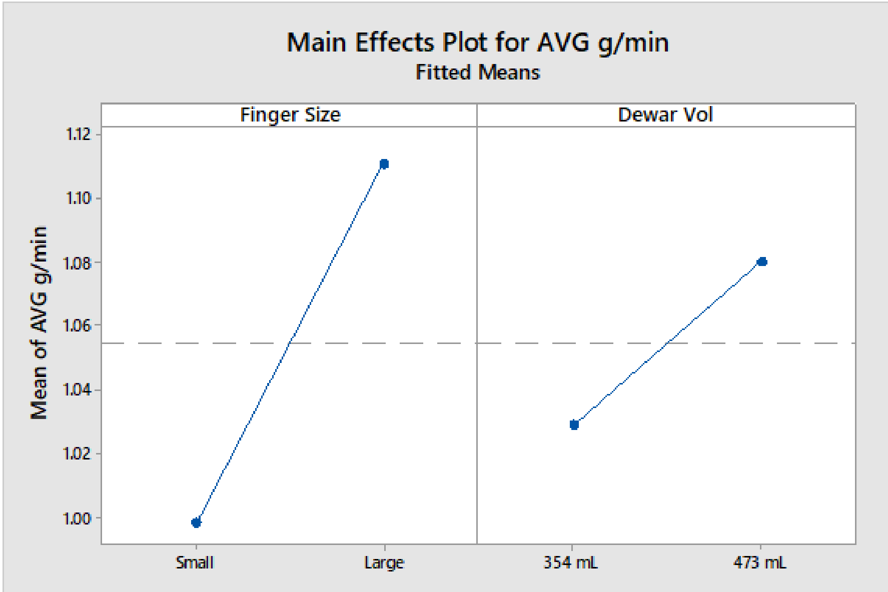

Figure 18. Main Effects Plot for Average Production Rate

Similar analysis was then conducted for the final liquid air production mass after 120 minutes of run time with a Pareto chart created in Minitab. Figure 19 shows that just the cold finger size was a critical and significant factor to the final produced mass of liquid air by crossing the reference line at 2.31. Again, the Dewar volume and the interaction of the cold finger size and the Dewar volume was determined to not be a critical factor as these fell below the reference line.

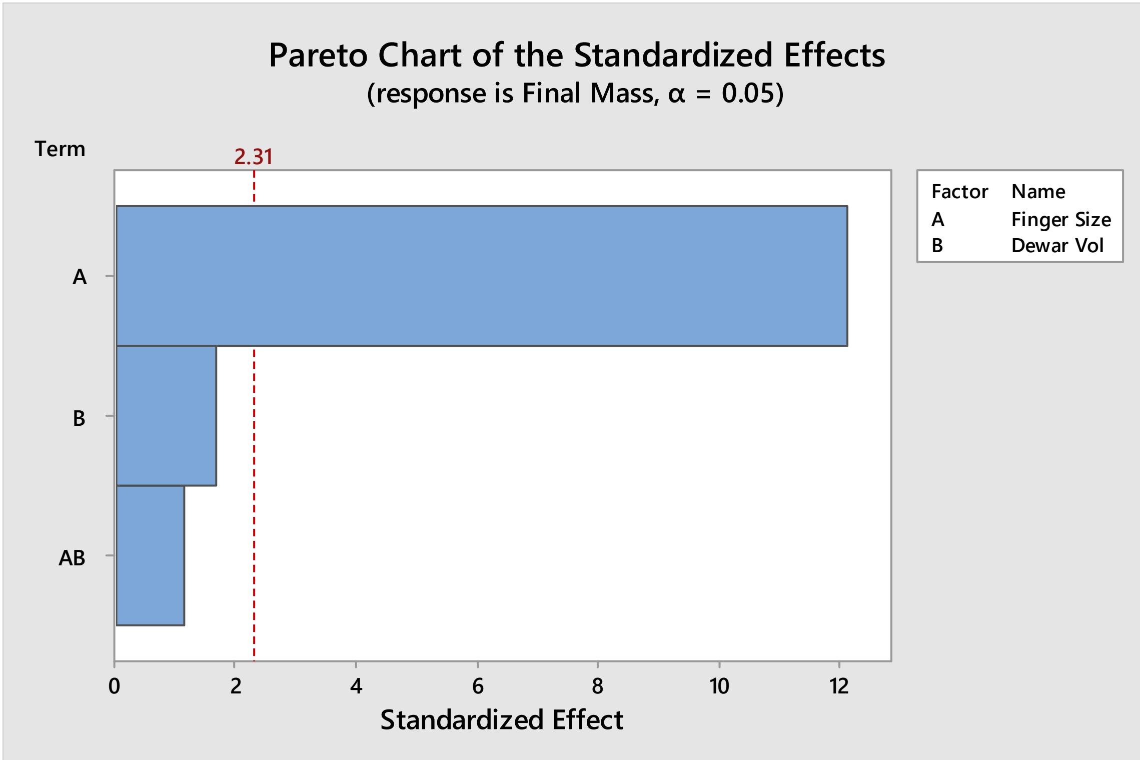

Figure 19. Final Production Mass Pareto Chart

An analysis of the ANOVA, two-factor with replication, Microsoft Excel table supported this finding as shown in Table 4. The hypothesis test asserts that the mean output measure is the same with the alternative being that there is some statistical difference between the measure means. In this instance, cold finger size results in an F-value of 146.5552. The probability that a value this extreme would be seen if the null hypothesis were true is the p-value of $2E^{-6}$. Because this probability is very small, and smaller than the significance level chosen, we state that the cold finger size factor is statistically significant and will influence the output measure.

Table 4. ANOVA Table for Final Production Mass

ANOVA					
Source of Variation	*SS*	*df*	*MS*	*F*	*P-value*
Finger size	4912.65	1	4912.653	146.5552	2E-06
Dewar Volume	95.2033	1	95.20333	2.840124	0.130427
Interaction	44.8533	1	44.85333	1.338073	0.280745
Within	268.167	8	33.52083		
Total	5320.88	11			

Figure 20 shows a main effects plot generated in Minitab to examine the direction of each factor. The plot shows that as the cold finger size is increased, the final production mass of liquid air will be lower. Alternatively, as the Dewar volume is increased, there will be a slight increase in the final production volume of liquid air but not a statistically significant amount. Therefore, if the maximum final production volume of this experimental setup would be desired, the smaller cold finger would be selected.

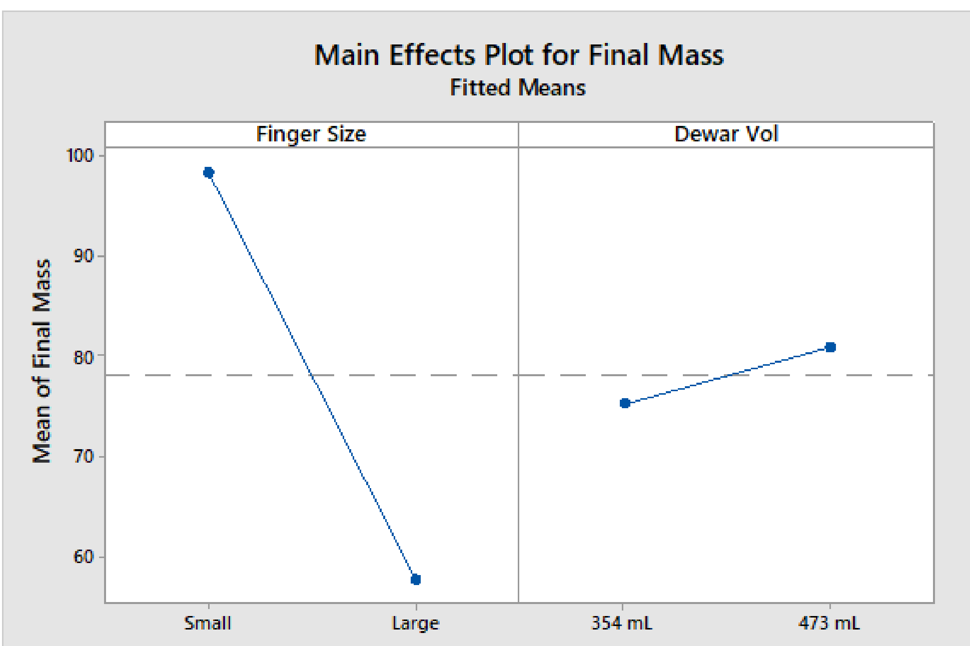

Figure 20. Main Effects Plot for Final Production Volume

Analyzing the time to when the system created its first gram of liquid air also provides insight into the system's effectiveness. Using Minitab, the Pareto chart for this response was generated as shown in Figure 21. The chart shows that cold finger size was a very significant factor and the only critical factor relative to the time the first gram of liquid air was produced.

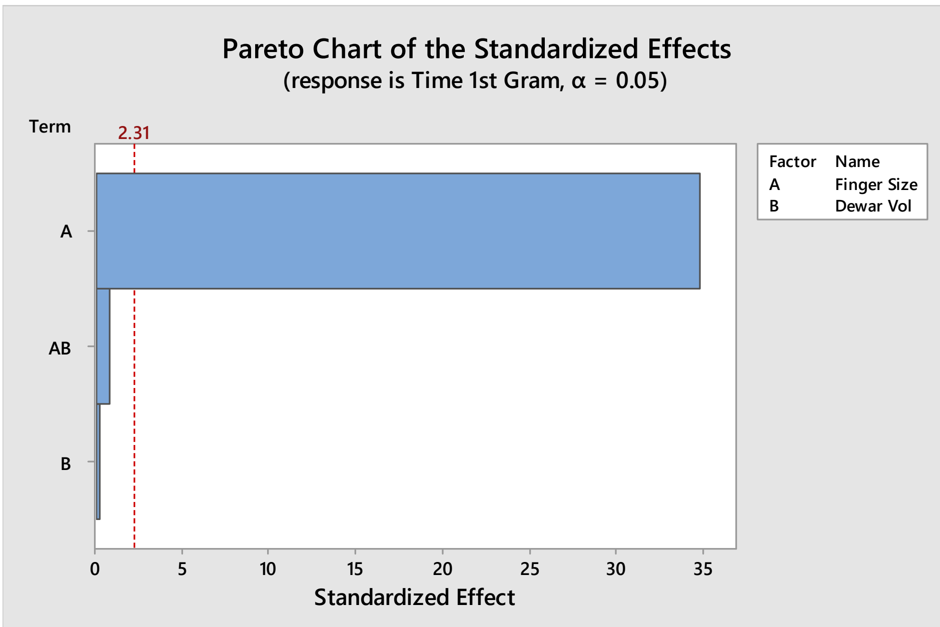

Figure 21. Time to First Gram Pareto Chart

The other factor of Dewar volume or the interaction between the two factors was not shown to be critical. Examining the direction of each factor with a main effects plot in Minitab as shown in Figure 22 support this analysis. The plot shows that as the cold finger size increases, then the time to produce the first gram of liquid air significantly increases as indicated by the steep slope of the cold finger size portion of the chart. The Dewar volume portion of Figure 22 also corresponds and supports the finding in Figure 21 as changes in the Dewar volume had no statistically significant impact on the time to first gram produced.

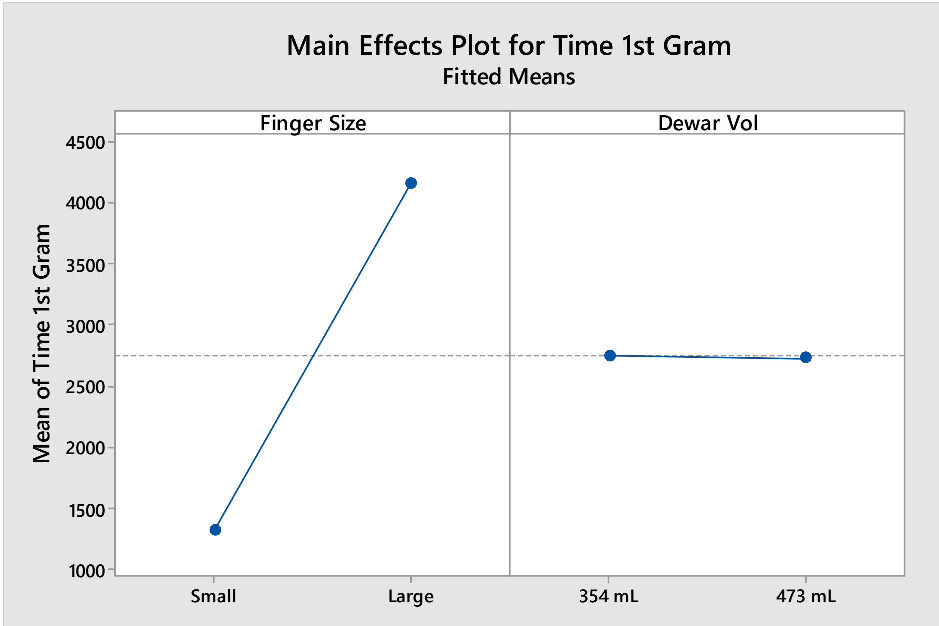

Figure 22. Main Effects Plot for Time to First Gram

The analysis of the time to first gram produced differs slightly from the findings for the other factors. The Pareto Chart shown in Figure 23 shows that the most statistically significant factor was the cold finger size with the Dewar volume also be statistically significant but to a lesser degree.

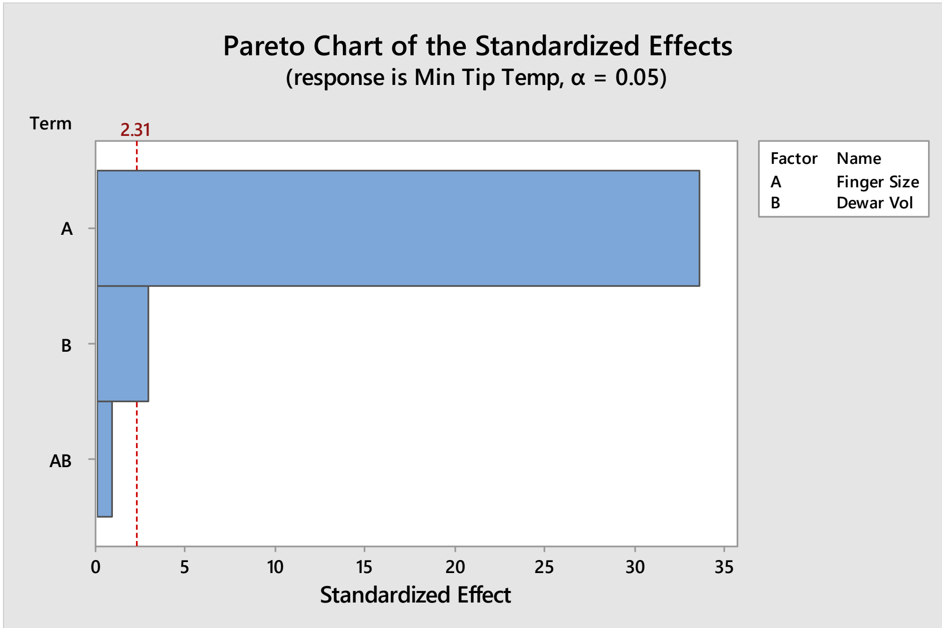

Figure 23. Minimum Tip Temperature Pareto Chart

Evaluating the direction of each factor, the main effects plot for the minimum cold tip temperature is shown in Figure 24. The plot shows that as the cold finger size increases, then the minimum temperature the system is able to generate in the experiment's two-hour time period is higher. The Dewar volume portion of Figure 24 also shows that the larger Dewar supports a lower temperature for the cryocooler's cold finger but within a much reduced range when compared to the cold finger size. Considering the finding in the analysis of time to first gram produced, the higher temperatures found in the larger cold finger extension correspond with the significant size and mass of the larger cold finger. Compared to the smaller cold finger extension, a larger body such as the large cold finger extension will take longer to cool than a smaller body, all other factors being equal.

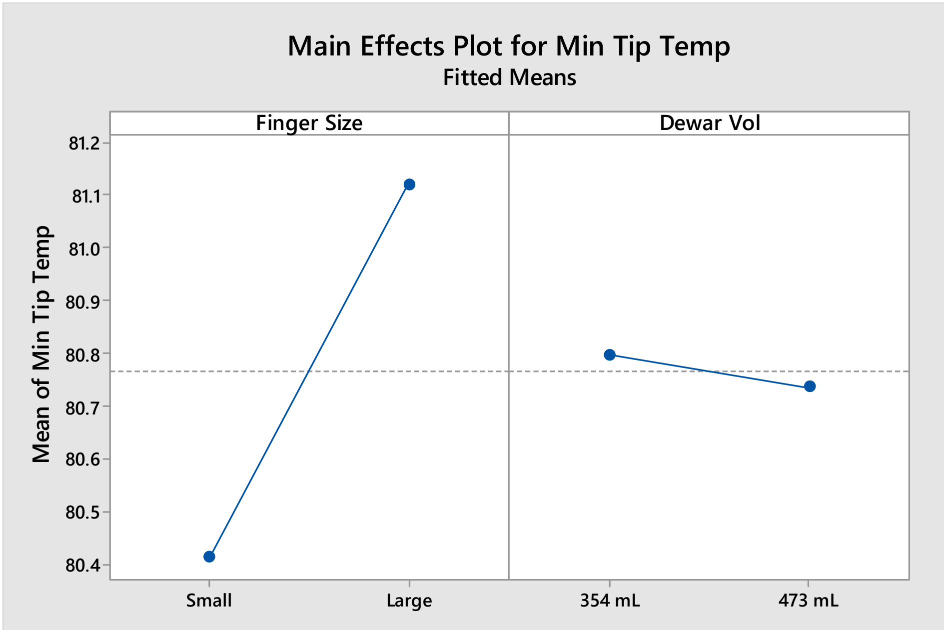

Figure 24. Main Effects Plot for the Minimum Tip Temperature

This analysis can then be condensed into a summary view shown in Table 5 to provide a clear picture of the results due to these factors.

Table 5. Analysis Summary

		Response			
		AVG Production Rate	**Final Mass**	**Time to 1st Gram Produced**	**Min Tip Temperature**
Factor	**Finger Size**	Significant	Significant	Significant	Significant
	Impact	Increasing size increases average production	Decreasing size increases final volume	Decreasing size decreases the time to first gram produced	Decreasing size lowers the minimum temperature the tip can reach
	Dewar Vol	Not Significant	Not Significant	Not Significant	Less Significant
	Impact	N/A	N/A	N/A	Increasing the size lowers the minimum temperature the tip can reach

The table reveals the cryocooler's cold finger size is a very significant factor in all responses measured. Increasing the size of the cold finger results in higher average production rates due to the larger surface area available to cool the air in the Dewar. The larger cold finger also results in increased time to the first gram of liquid air produced due to the larger cold finger's increased mass taking longer to reach the temperature where liquid air is produced. Increasing the size of the cold finger also limits the minimum cold tip temperature when operated for only two hours as compared to the smaller cold finger due to the larger mass of the large cold finger still cooling down. This combination of factors results in a lower final volume of liquid air produced over a two-hour period compared to a smaller cold finger. The Dewar volume was found to be a significant factor in only the minimum temperature the cold tip can achieve. The analysis shows that increasing the Dewar volume would result in lower minimum cold tip temperatures over two hours of operation. However, the response to this factor was significantly less than the response to the changes in cold finger size. These findings support design criteria for future engineering efforts on the NPS LAES microgrid system.

THIS PAGE INTENTIONALLY LEFT BLANK

IV. CONCLUSION, RECOMMENDATIONS, AND FUTURE WORK

This thesis analyzed the significance of a cryocooler’s cold finger surface area and Dewar volume as part of a component design for a LAES system supporting ongoing analysis of microgrid technologies in the Turbo-Propulsion Laboratory at the Naval Postgraduate School. This effort applied the bottom of the system engineering V model to characterize and verify component design details before progressing along in the model to subsystem and system design for a microgrid system. A verification plan for these designs was laid out using a design of experiments to test and then evaluate the statistical significance to changes in these factors.

Through this effort, the experiments found that changing the characteristics of a cryocooler’s cold finger has a statistically significant impact on liquid air production rates, total production volume, time to first gram produced, and minimum cold finger temperature. On the other hand, changing the container size had only a slight effect on the minimum cold finger temperature. The implications of this analysis for a system’s engineer considering a liquid air production system design would, therefore, mainly focus on the factor of cryocooler cold finger design based on the significant impact of this factor.

Overall, LAES systems are a favorable energy storage technology for a mobile microgrid structure due to their high energy density, high round-trip efficiencies, use of common industrial materials, and no geographic limitations that are inherent to other storage technologies. The incorporation of LAES into renewable energy microgrid structures mitigates the characteristic problem of renewable energy’s intermittent generation and the need to move excess power from low demand times to high demand times to support a continuous electrical supply. In turn, this supports the DOD’s focus on energy resilience, conservation, and a reduced logistical burden from tradition fossil fuel derived energy generation methods.

A. RECOMMENDATION

An evaluation of a LAES system requirements, operating environment, and stakeholder needs along with the analysis in this thesis would help guide a system engineer based on the following recommendations. If fast liquid air production startup was determined to be a desired system attribute because of short excess power availability or many intermittent power intervals, then a cryocooler design that takes advantage of a smaller cold finger extension would minimize the cool down time for the system. The DOE found that this would result in a lower average production volume rate but would start to produce liquid air much sooner by reaching the condensation point faster. Therefore, if the system would only operate for a limited time, then liquid air production would be maximized by starting production sooner rather than trying to maximize the average production rate.

Alternatively, if an evaluation of a system's operating environment indicated that longer excess power intervals were normal, then there could be a benefit to the greater surface area of a larger cryocooler cold finger as it increases average production rates. However, as indicated in the DOE, this increase in average production would come at the expense of a longer startup time. The DOE revealed that the larger cryocooler cold finger extension was not able to achieve the same minimum temperature as a smaller cold finger extension; however, that analysis was purely in the context of a fixed two hour time block of operation for the experimentation in this thesis. In evaluating the last 40 minutes of run time data for the cold finger temperature, all runs were continuing to decrease in temperature and had not stabilized at their steady-state temperature. Therefore, it is believed that a larger cryocooler cold finger extension would still permit reaching the desired temperature of 79 K to full liquefy all primary elements of atmospheric air. This theory supports the assertion that this type of subsystem design would be more beneficial in a system that would be expected to have longer run times to account for the slower cool down characteristics but take advantage of larger average production rates.

B. FUTURE WORK

Future work on LAES systems could include control systems that optimize the generation of liquid air production based on environmental conditions or forecasts, an evaluation of the energy recovery side of a LAES using a Stirling engine, or continued improvements of the cold finger extension. Considering that this work only analyzed one aspect of cryocooler cold finger design, other variables could significantly impact liquid air production to include changing materials, improving contact between the cold finger and the extension, or different physical designs for the cold finger extension similar to common heat exchanger designs.

THIS PAGE INTENTIONALLY LEFT BLANK

APPENDIX. DATA

Experiment	Small	**Dewar**	Hydro Flask
Run Number	1	**Size (mL)**	354
Ambient Temp (K)	299.75	**Mass (g)**	225.7
Power Setting (W)	240		
Time to first gram (sec)	1487	24 min 47 sec	
Time	**Tip Temp (K)**	**Liquid Mass (g)**	
0	302.01	0	
10	113.66	0	
20	81.06	0	
30	80.82	5.1	
40	80.72	14.5	
50	80.67	23.9	
60	80.64	33.3	
70	80.66	42.8	
80	80.58	52.2	
90	80.54	61.6	
100	80.5	71	
110	80.47	80.3	
120	80.46	89.7	

Experiment	Small	**Dewar**	Hydro Flask
Run Number	2	**Size (mL)**	354
Ambient Temp (K)	298.25	**Mass (g)**	225.7
Power Setting (W)	240		
Time to first gram (sec)	1453	24 min 13 sec	
Time	**Tip Temp (K)**	**Liquid Mass (g)**	
0	300.18	0	
10	112.13	0	
20	81.06	0	
30	80.89	6	
40	80.87	15	
50	80.77	23.6	
60	80.7	32.6	
70	80.63	41.8	
80	80.55	51.1	
90	80.52	60.8	
100	80.48	69.8	
110	80.45	78.9	
120	80.44	88.2	

Experiment	Small	**Dewar**	Hydro Flask
Run Number	3	**Size (mL)**	354
Ambient Temp (K)	299.25	**Mass (g)**	225.7
Power Setting (W)	240		
Time to first gram (sec)	1148	19 min 08 sec	
Time	**Tip Temp (K)**	**Liquid Mass (g)**	
0	301.05	0	
10	113.74	0	
20	80.83	2.1	
30	80.6	12.1	
40	80.53	22.1	
50	80.47	32	
60	80.42	42.1	
70	80.57	52.3	
80	80.49	62.3	
90	80.47	72.3	
100	80.45	82.2	
110	80.42	92.3	
120	80.4	102.6	

Experiment	Large	**Dewar**	Hydro Flask
Run Number	1	**Size (mL)**	354
Ambient Temp (K)	301.25	**Mass (g)**	225.7
Power Setting (W)	240		
Time to first gram (sec)	4225	70 min 25 sec	
Time	**Tip Temp (K)**	**Liquid Mass (g)**	
0	304.58	0	
10	253.98	0	
20	208.94	0	
30	167.17	0	
40	134.7	0	
50	108.63	0	
60	90.2	0	
70	81.31	0.9	
80	81.21	12	
90	81.18	23.2	
100	81.16	34.4	
110	81.15	45.7	
120	81.14	56.9	

Experiment	Large	**Dewar**	Hydro Flask
Run Number	2	**Size (mL)**	354
Ambient Temp (K)	299.15	**Mass (g)**	225.7
Power Setting (W)	240		
Time to first gram (sec)	4231	70 min 31 sec	
Time	**Tip Temp (K)**	**Liquid Mass (g)**	
0	301.41	0	
10	246.51	0	
20	198.2	0	
30	156.68	0	
40	123.19	0	
50	97.15	0	
60	81.42	0	
70	81.2	0	
80	81.16	11	
90	81.17	22	
100	81.17	32.9	
110	81.15	43.9	
120	81.13	54.9	

Experiment	Large	**Dewar**	Hydro Flask
Run Number	3	**Size (mL)**	354
Ambient Temp (K)	296.45	**Mass (g)**	225.7
Power Setting (W)	240		
Time to first gram (sec)	3967	66 min 7 sec	
Time	**Tip Temp (K)**	**Liquid Mass (g)**	
0	298.78	0	
10	242.82	0	
20	195.17	0	
30	154.5	0	
40	122.23	0	
50	97.45	0	
60	81.7	0	
70	81.25	4.9	
80	81.23	15.7	
90	81.22	26.6	
100	81.22	37.4	
110	81.23	48.1	
120	81.21	58.9	

Experiment	Small	**Dewar**	Hydro Flask
Run Number	1	**Size (mL)**	473
Ambient Temp (K)	299.45	**Mass (g)**	230.1
Power Setting (W)	240		
Time to first gram (sec)	1340	22 mins 20 sec	
Time	**Tip Temp (K)**	**Liquid Mass (g)**	
0	301.55	0	
10	115.02	0	
20	81.05	0	
30	80.75	7	
40	80.67	18	
50	80.6	28.2	
60	80.5	38.6	
70	80.51	49	
80	80.48	59.5	
90	80.43	70	
100	80.42	80.5	
110	80.38	91.1	
120	80.36	101.8	

Experiment	Small	**Dewar**	Hydro Flask
Run Number	2	**Size (mL)**	473
Ambient Temp (K)	297.65	**Mass (g)**	230.1
Power Setting (W)	240		
Time to first gram (sec)	1187	19 min 47 sec	
Time	**Tip Temp (K)**	**Liquid Mass (g)**	
0	299.89	0	
10	112.5	0	
20	80.9	1.2	
30	80.71	11.7	
40	80.6	22.1	
50	80.53	32.5	
60	80.52	42.8	
70	80.52	53.2	
80	80.49	63.6	
90	80.45	74.1	
100	80.42	84.5	
110	80.41	94.9	
120	80.39	105.2	

Experiment	Small	**Dewar**	Hydro Flask
Run Number	3	**Size (mL)**	473
Ambient Temp (K)	296.65	**Mass (g)**	230.1
Power Setting (W)	240		
Time to first gram (sec)	1294	21 min 34 sec	
Time	**Tip Temp (K)**	**Liquid Mass (g)**	
0	298.89	0	
10	109.97	0	
20	80.84	0	
30	80.69	10.1	
40	80.6	20.3	
50	80.57	30.5	
60	80.59	40.8	
70	80.57	51	
80	80.54	61.2	
90	80.5	71.4	
100	80.46	81.6	
110	80.45	91.8	
120	80.42	102	

Experiment	Large	**Dewar**	Hydro Flask
Run Number	1	**Size (mL)**	473
Ambient Temp (K)	297.65	**Mass (g)**	230.1
Power Setting (W)	240		
Time to first gram (sec)	4323	72 min 3 sec	
Time	**Tip Temp (K)**	**Liquid Mass (g)**	
0	299.51	0	
10	244.31	0	
20	197.05	0	
30	156.76	0	
40	124.16	0	
50	98.96	0	
60	82.05	0	
70	81.17	0	
80	81.13	10.4	
90	81.11	20.9	
100	81.1	31.6	
110	81.1	42.5	
120	81.08	53	

Experiment	Large	**Dewar**	Hydro Flask
Run Number	2	**Size (mL)**	473
Ambient Temp (K)	297.95	**Mass (g)**	230.1
Power Setting (W)	240		
Time to first gram (sec)	4186	69 mins 46 sec	
Time	**Tip Temp (K)**	**Liquid Mass (g)**	
0	299.82	0	
10	245.3	0	
20	198.76	0	
30	157.84	0	
40	125.49	0	
50	100.12	0	
60	82.7	0	
70	81.19	1.2	
80	81.17	11.9	
90	81.16	22.7	
100	81.15	33.6	
110	81.13	44.4	
120	81.12	55.2	

Experiment	Large	**Dewar**	Hydro Flask
Run Number	3	**Size (mL)**	473
Ambient Temp (K)	296.55	**Mass (g)**	230.1
Power Setting (W)	240		
Time to first gram (sec)	4064	67 min 44 sec	
Time	**Tip Temp (K)**	**Liquid Mass (g)**	
0	299.04	0	
10	245.13	0	
20	196.89	0	
30	155.28	0	
40	122.09	0	
50	96.68	0	
60	81.35	0	
70	81.15	7.2	
80	81.11	19.2	
90	81.08	31.3	
100	81.05	43.4	
110	81.06	55.6	
120	81.04	67.8	

LIST OF REFERENCES

Amalla, Sammy. 2019. "Construction, Operation, and Design Improvement of a Small-Scale Liquid Air Energy Storage System Prototype." Master's thesis, Naval Postgraduate School. http://hdl.handle.net/10945/62837.

Bailey, Nicholas A. 2019. "Model-Based Simulation, Analysis, and Prototyping for Future Liquid Air Energy Storage Systems." Master's thesis, Naval Postgraduate School. https://calhoun.nps.edu/handle/10945/64028.

Bailey, Nicholas A., Anthony G. Pollman, and Eugene P. Paulo. 2020. "Energy Recovery for Dual-Stirling Liquid Air Energy Storage Prototype." In *ASME 2020 Power Conference*, V001T10A002. Virtual, Online: American Society of Mechanical Engineers. https://doi.org/10.1115/POWER2020-16087.

Eady, Davis S., Steven B. Siegel, Steven Bell, and Scott H. Dicke. 2009. *Sustain the Mission Project: Casualty Factors for Fuel and Water Resupply Convoys*. Technical Report. Arlington, Va: Army Environmental Policy Institute. https://apps.dtic.mil/dtic/tr/fulltext/u2/b356341.pdf.

Forsberg, Kevin, and Harold Mooz. 1992. "The Relationship of Systems Engineering to the Project Cycle." *Engineering Management Journal* 4 (3): 36–43. https://doi.org/10.1080/10429247.1992.11414684.

Fu, Ran, Timothy Remo, and Robert Margolis. 2018. *2018 U.S. Utility-Scale Photovoltaics-Plus-Energy Storage System Costs Benchmark*. National Renewable Energy Laboratory. Golden, CO: U.S. Department of Energy. https://www.nrel.gov/docs/fy19osti/71714.pdf.

Gannon, Anthony. 2017. "ESTEP Research Project Spotlight: NPS TurboProp Lab Microgrid." https://calhoun.nps.edu/handle/ 10945/60010.

Gannon, Anthony. 2018. "Energy Solutions: A New Energy System Design Approach [Video]." Naval Postgraduate School, Monterey, California. 1.08:31. https://calhoun.nps.edu/handle/10945/59069.

Girouard, Christopher M. 2019. "Model-Based and Experimental Analysis for Future Liquid Air Energy Storage Systems." Master's thesis, Naval Postgraduate School. https://calhoun.nps.edu/handle/10945/64166.

Girouard, Christopher, Anthony G Pollman, and Alejandro Hernandez. 2019. "Modeling and Simulation Informed Conceptual Design, Analysis, and Initial Component Selection of a Supply-Side Building Scale LAES System for Renewable, Islanded Microgrid Resiliency." In *MORS Symposium*, 14. Colorado Springs, CO. https://calhoun.nps.edu/bitstream/handle/10945/65186/Girouard-Pollman-Hernandez_MORSPaperFinal.pdf?sequence=1&isAllowed=y.

Greenley, Heather L. 2019. *Department of Defense Energy Management: Background and Issues for Congress*. CRS Report No. R45832. Washington, DC: Congressional Research Service. https://fas.org/sgp/crs/natsec/R45832.pdf.

Halliday, David, Rober Resnick, and Jearl Walker. 2014. *Fundamentals of Physics*. 10th ed. Danvers, MA: John Wiley & Sons, Inc.

Hawxhurst, Kevin, Joshua Williams, Anthony Pollman, and Anthony Gannon. 2017. “Renewable-Powered HVAC with Thermal Storage.” *ASHRAE Journal* 59 (12): 21–27.

Howe, Todd A. 2018. “Thermodynamic System Analysis of a Liquid Air Energy Storage System.” Master’s thesis, Naval Postgraduate School. https://calhoun.nps.edu/bitstream/handle/10945/59687/18Jun_Howe_Todd_Needs_Supplemental.pdf?sequence=1&isAllowed=y.

Howe, Todd, Anthony Pollman, and Anthony Gannon. 2018. “Operating Range for a Combined, Building-Scale Liquid Air Energy Storage and Expansion System: Energy and Exergy Analysis.” *Entropy* 20 (10): 770. https://doi.org/10.3390/e20100770.

Ibrahim, H, A Ilinca, and J Perron. 2008. “Energy Storage Systems—Characteristics and Comparisons.” *Renewable and Sustainable Energy Reviews* 12 (5): 1221–50. https://doi.org/10.1016/j.rser.2007.01.023.

J Scales. 2020. *CJ-Series User Manual*. Accessed September 21, 2020. https://jscale.com/portfolio/cj600/.

Jung, Lisa A. 2020. “Fiscal Years 2022 and 2023 Energy Resilience and Conservation Investment Program Guidance.” Official memorandum. Washington, DC: Department of Defense. https://www.acq.osd.mil/eie/IE/FEP_ECIP.html.

Kim, Young-Min, Jang-Hee Lee, Seok-Joon Kim, and Daniel Favrat. 2012. “Potential and Evolution of Compressed Air Energy Storage: Energy and Exergy Analyses.” *Entropy* 14 (August): 1501–21. https://doi.org/10.3390/e14081501.

Kohler, J.W.L. 1965. “The Stirling Refrigeration Cycle.” *Scieentific American* 212 (4): 119–27.

Krawczyk, Piotr, Łukasz Szabłowski, Sotirios Karellas, Emmanuel Kakaras, and Krzysztof Badyda. 2016. “Comparative Energy and Exergy Analysis of Compressed Air and Liquid Air Energy Storage Systems.” In *International Conference on Efficiency, Cost, Optimization, Simulation and Environmental Impact of Energy Systems*, 1–11. Portoroz, Slovenia.

Law, Averill. 2015. *Simulations Modeling and Analysis*. 5th ed. New York, NY: McGraw-Hill Education.

Morgan, R.E. 2016. "Liquid Air Energy Storage – from Theory to Demonstration." *International Journal of Environmental Studies* 73 (May): 469–80. https://doi.org/10.1080/00207233.2016.1189741.

Narayanan, Anu, Jonathan Welburn, Benjamin Miller, Sheng Li, and Aaron Clark-Ginsberg. 2020. *Deterring Attacks Against the Power Grid: Two Approaches for the U.S. Department of Defense*. RAND Corporation. https://doi.org/10.7249/RR3187.

Pollman, Anthony G. 2013. "Energy Optimization: A Combat Multiplier." *Marine Corps Gazette*, November 2013.

Pollman, Anthony G., and Anthony J. Gannon. 2015. "Multi-Physics Energy Approach and Demonstration Facility." In *ASME 2015 9th International Conference on Energy Sustainability Collocated with the ASME 2015 Power Conference, the ASME 2015 13th International Conference on Fuel Cell Science, Engineering and Technology, and the ASME 2015 Nuclear Forum*, V001T03A001. San Diego, California, USA: American Society of Mechanical Engineers. https://doi.org/10.1115/ES2015-49084.

Rcharlance. 2020. "Rcharlance 150A RC Watt Meter Power Analyzer High Precision FT08 Battery Voltage Amp Meter with Backlight LCD Balancer 60VModel Tester." Accessed September 21, 2020. https://www.amazon.com/Rcharlance-Analyzer-Precision-Backlight-Balancer/dp/B07DL3MY21/ref=sr_1_2?dchild=1&keywords=inline+150A+power+monitor&qid=1600706062&sr=8-2.

Schroeder, Daniel V. 2000. *An Introduction to Thermal Physics*. Internat. ed. San Francisco, Calif.: Addison Wesley.

Shaw, John E. 2008. "Comparing Carnot, Stirling, Otto, Brayton and Diesel Cycles." *Transactions of the Missouri Academy of Science* 42 (2008): 1–6. https://doi.org/10.30956/0544-540X-42.2008.1.

Sunpower Inc. 2016. *Installation and Operation Manual Rev. 8 for the CryoTel GT Cryocooler and Gen II Controller*. Athens, OH. https://www.sunpowerinc.com/products/stirling-cryocoolers/cryotel-cryocoolers/gt.

Wald, Charles F., and Tom Captain. 2009. *Energy Security America's Best Defense*. Study. Deloitte Development LLC. https://www.offiziere.ch/wp-content/uploads/us_ad_EnergySecurity052010.pdf.

Willis, Ryan. 2019. "Modeling of a Building- Scale Liquid Air Energy Storage System with ASPEN HYSYS." Master's Thesis, Naval Postgraduate School. http://hdl.handle.net/10945/63519.

THIS PAGE INTENTIONALLY LEFT BLANK

INITIAL DISTRIBUTION LIST

1. Defense Technical Information Center
   Ft. Belvoir, Virginia

2. Dudley Knox Library
   Naval Postgraduate School
   Monterey, California